THE PLANT CELL

Research Article

Cross-talk between clathrin-dependent post-Golgi trafficking and clathrin-mediated endocytosis in Arabidopsis root cells

Xu Yan [1,*,‡] Yutong Wang [1,‡] Mei Xu [1,‡] Dana A. Dahhan [2] Chan Liu [1] Yan Zhang [3] Jinxing Lin [4] Sebastian Y. Bednarek [2,*,†] and Jianwei Pan [1]

1 Ministry of Education Key Laboratory of Cell Activities and Stress Adaptations, School of Life Sciences, Lanzhou University, Lanzhou 730000, China
2 Department of Biochemistry, University of Wisconsin–Madison, Madison, Wisconsin 53706
3 State Key Laboratory of Crop Biology, College of Life Sciences, Shandong Agricultural University, Tai'an 271018, China
4 College of Biological Sciences and Biotechnology, Beijing Forestry University, Beijing 100083, China

*Author for correspondence: sybednar@wisc.edu (S.Y.B.), yanx18@lzu.edu.cn (X.Y.).
†Senior author.
‡These authors contributed equally to this work.

X.Y., Y.W., M.X., D.A.D., Y.Z., J.L., S.Y.B., and J.P. conceived the study and designed the experiments. X.Y., Y.W., M.X., and C.L. carried out the experiments. X.Y., Y.W., M.X., J.L., S.Y.B., and J.P. analyzed the data. X.Y., Y.W., M.X., J.P. and S.Y.B. wrote the article. S.Y.B., D.A.D., X.Y., and Y.W. revised the manuscript.

The authors responsible for distribution of materials integral to the findings presented in this article in accordance with the policy described in the Instructions for Authors (https://academic.oup.com/plcell) are: Sebastian Y. Bednarek (sybednar@wisc.edu) and Xu Yan (yanx18@lzu.edu.cn).

Abstract

Coupling of post-Golgi and endocytic membrane transport ensures that the flow of materials to/from the plasma membrane (PM) is properly balanced. The mechanisms underlying the coordinated trafficking of PM proteins in plants, however, are not well understood. In plant cells, clathrin and its adaptor protein complexes, AP-2 and the TPLATE complex (TPC) at the PM, and AP-1 at the trans-Golgi network/early endosome (TGN/EE), function in clathrin-mediated endocytosis (CME) and post-Golgi trafficking. Here, we utilized mutants with defects in clathrin-dependent post-Golgi trafficking and CME, in combination with other cytological and pharmacological approaches, to further investigate the machinery behind the coordination of protein delivery and recycling to/from the TGN/EE and PM in Arabidopsis (*Arabidopsis thaliana*) root cells. In mutants with defective AP-2-/TPC-dependent CME, we determined that clathrin and AP-1 recruitment to the TGN/EE as well as exocytosis are significantly impaired. Likewise, defects in AP-1-dependent post-Golgi trafficking and pharmacological inhibition of exocytosis resulted in the reduced association of clathrin and AP-2/TPC subunits with the PM and a reduction in the internalization of cargoes via CME. Together, these results suggest that post-Golgi trafficking and CME are coupled via modulation of clathrin and adaptor protein complex recruitment to the TGN/EE and PM.

Introduction

Post-Golgi secretory and endocytic vesicle trafficking pathways control the delivery and retrieval of proteins and membranes from the cell surface and thereby regulate cell growth and numerous biochemical processes at the plasma membrane (PM) essential for the interaction and exchange of information between a cell and its environment. Clathrin, an evolutionarily conserved vesicle coat protein complex, which localizes to the PM and trans-Golgi network/early

Open Access

IN A NUTSHELL

Background: The plasma membrane separates the inside of cells from the outside environment, thereby regulating the entry and exit of molecules and signals to and from cells. Proteins that function at the plasma membrane are produced and modified within cellular "factories", the endoplasmic reticulum and the Golgi apparatus, prior to their delivery from the main "distribution center" in the cell, the *trans*-Golgi network/early endosome (TGN/EE), to the cell surface via a process called exocytosis. Simultaneously, cell surface proteins are internalized through endocytosis to the TGN/EE from which they can be re-distributed back to the plasma membrane or to the vacuole for degradation. The mechanisms that coordinate exocytosis and endocytosis to regulate the levels of plasma membrane proteins are unknown. However, plant genomes do encode components of the clathrin and AP-1 adaptor complexes, which are critical for the budding of vesicles from membranes.

Question: Is the recruitment of clathrin and clathrin-associated proteins involved in exocytosis from the TGN/EE and in endocytosis from the plasma membrane coordinately regulated?

Findings: Disruption of clathrin-mediated endocytosis in the model plant *Arabidopsis thaliana* reduced the association of clathrin and the adaptor protein AP-1 with the TGN/EE, thereby inhibiting trafficking of plasma membrane proteins from the TGN/EE. In turn, genetic disruption of AP-1 function or chemical inhibition of exocytosis inhibited the plasma membrane association of the AP-2 adaptor protein and the TPLATE complex, resulting in reduced clathrin-mediated endocytosis. These results strongly indicate that endocytosis and exocytosis are coupled in plant cells through the membrane recruitment of clathrin and its adaptor proteins to the TGN/EE and plasma membrane.

Next steps: The signaling mechanisms that coordinate clathrin-dependent endocytosis and exocytosis pathways need to identified.

endosome (TGN/EE) ([Konopka et al., 2008](); [Ito et al., 2012]()), plays a critical role in post-Golgi exocytic/endocytic routes that control the abundance and activity of PM proteins ([Lam et al., 2007](); [McMahon and Boucrot, 2011](); [Kirchhausen et al., 2014](); [Zouhar and Sauer, 2014](); [Kukulski et al., 2016](); [Kaksonen and Roux, 2018](); [Reynolds et al., 2018]()).

Binding of clathrin to the PM or TGN/EE is dependent upon membrane compartment-specific adaptor protein complexes that, together with clathrin, recruit additional accessory proteins necessary for the formation, cargo recognition, budding, and release of cargo-containing clathrin-coated vesicles (CCVs) ([McMahon and Boucrot, 2011](); [Paez Valencia et al., 2016](); [Kaksonen and Roux, 2018]()). Clathrin-mediated endocytosis (CME) in plants is dependent upon various endocytic accessory proteins, including two types of adaptor protein complexes: the evolutionarily conserved heterotetrameric complex ADAPTOR PROTEIN2 (AP-2, consisting of AP2α, AP2β, AP2μ, and AP2σ), and the evolutionarily ancient heterooctameric TPLATE complex (TPC) ([Kim et al., 2013](); [Yamaoka et al., 2013](); [Gadeyne et al., 2014](); [Zhang et al., 2015]()). Following budding and release from the PM, cargo-containing plant CCVs uncoat in close proximity to the TGN/EE, rather than immediately after scission from the PM ([Narasimhan et al., 2020]()). Within the TGN/EE, PM proteins are either recycled back to the PM or targeted through intermediate/late endosomes (termed multivesicular bodies; MVBs) for vacuolar degradation. In addition to PM cargoes, endosomes also receive secretory proteins translated de novo and fated for the vacuole.

The ADAPTOR PROTEIN1 complex (AP-1, consisting of AP1γ, AP1β, AP1μ, and AP1σ) functions in clathrin-dependent sorting and trafficking between the TGN and endosomes ([Castillon et al., 2018](); [Martzoukou et al., 2018]()). However, AP-1 has also been implicated in the polarized sorting of PM proteins in epithelial and neuronal cells ([Gravotta et al., 2012](), [2019](); [Li et al., 2016]()) as well as intra-Golgi recycling of secretory cargoes and Golgi-resident proteins ([Papanikou et al., 2015](); [Day et al., 2018](); [Casler et al., 2019]()).

In plants, morphometric studies have estimated that $\geq$75% of the total membrane incorporated into the PM of an expanding cell or cell plate during cytokinesis is recycled by endocytosis ([Otegui and Staehelin, 2000](); [Otegui et al., 2001]()). Therefore, the coordination of exocytic and endocytic trafficking is critical to regulate cell surface area as well as PM protein abundance and activity ([Zhang et al., 2019]()). Components of the endocytic machinery, including clathrin, are necessary in plants and animals for the process of exocytosis ([Jaiswal et al., 2009](); [Kawasaki et al., 2011](); [Larson et al., 2017]()). Furthermore, disruption of the exocyst complex or the function of SNAREs (exocytic soluble *N*-ethylmaleimide-sensitive factor attachment protein receptors), which are required for secretory vesicle tethering and fusion with the PM, respectively, inhibits endocytosis ([Wu et al., 2005](); [Jose et al., 2015](); [Boehm et al., 2017](); [Larson et al., 2017]()). However, the mechanisms that coordinate the activities of the post-Golgi exocytic and endocytic trafficking are poorly understood.

We previously demonstrated that loss or partial loss of function of the CME adaptor protein complexes, AP-2 or

TPC, results in a decrease in the levels of TGN/EE-associated clathrin (Wang et al., 2016a), suggesting that post-Golgi trafficking is modulated by CME. In this study, we show that defects in post-Golgi trafficking or CME affect the recruitment of clathrin and its accessory proteins to the TGN/EE and PM, thereby providing further evidence that the processes of exocytosis and endocytosis are coordinated/coupled in plant cells.

Results

Clathrin localization to the TGN/EE depends on AP-1

To examine whether the function of AP-1 is necessary for clathrin localization to the TGN/EE, as observed in other systems (Burgess et al., 2011; Daboussi et al., 2012; Martzoukou et al., 2018), we established that subunits of the AP-1 complex and clathrin colocalize. As expected based on previous studies of the localization (Park et al., 2013; Teh et al., 2013; Wang et al., 2013a) and biochemical analysis of the AP-1 complex subunit composition (Teh et al., 2013), AP1μ2 tagged with red fluorescent protein (AP1μ2-RFP) and AP1σ2 subunits tagged with green fluorescent protein (AP1σ2-GFP) colocalized in Arabidopsis root cells at the TGN/EE (Supplemental Figure S1, A) as well as with GFP- or monomeric Kusabira-Orange fluorescent-tagged clathrin light chain 2 (CLC2-GFP or CLC2-mKO) (Supplemental Figure S1, B and C).

Next, we examined whether AP-1 is required for clathrin recruitment to the TGN/EE. For these studies, we used the previously characterized loss-of-function Arabidopsis ap1μ2 (hapless13) mutant (Park et al., 2013; Wang et al., 2013a, 2016b) as well as the ap1σ1-1 and ap1σ2-1 T-DNA insertion mutant lines, in which the expression of genes encoding AP1σ subunit isoforms, AP1σ1 and AP1σ2 is disrupted (Supplemental Figure S2). ap1σ1-1 and ap1σ2-1 seedlings, as well as seedlings with a single functional copy of either AP1σ1 or AP1σ2 (ap1σ1-1/AP1σ1 ap1σ2-1 and ap1σ1-1 ap1σ2-1/AP1σ2) exhibited no discernable phenotypes. By contrast, homozygous ap1σ1-1 ap1σ2-1 double mutant seedlings displayed a reduction in growth on half-strength Murashige and Skoog (MS) agar plates (Supplemental Figure S2, C) and loss of viability on soil after 2–3 weeks (Supplemental Figure S2, D), similar to the phenotype of ap1μ2 null mutants (Park et al., 2013; Teh et al., 2013; Wang et al., 2013a). The observed developmental defects in ap1σ1-1 ap1σ2-1 were rescued by the introduction of a 35Spro:AP1σ2-GFP transgene (Supplemental Figure S2, E). These data indicate the functional redundancy of AP1σ1 and AP1σ2 in plant growth and development.

As detected by quantitative immunofluorescence (IF) microscopy using affinity-purified anti-CLC1 and anti-CHC antibodies (Wang et al., 2013b; Supplemental Table S2), loss of AP1μ2, or AP1σ1 and AP1σ2, resulted in a ∼40%–60% reduction in the levels of TGN/EE-associated clathrin (Figure 1, A–D). Likewise, live-cell imaging showed that fluorescence intensity at the TGN/EE derived from the Arabidopsis CHC isoforms, CHC1 and CHC2, and the three CLC isoforms,

CLC1, CLC2, and CLC3, tagged with GFP, decreased by ∼55%–60% (CHCs) and ∼50%–60% (CLCs) in ap1μ2 relative to the WT (Supplemental Figure S3, A–O).

Given that homozygous ap1μ2 and ap1σ1 ap1σ2 double mutant seedlings exhibited major defects in growth and development (Supplemental Figure S2), we examined whether clathrin localization is also affected in less severe ap-1 RNA interference (RNAi) lines. For these studies, we used previously described transgenic lines in which the levels of AP1μ2 transcript are reduced by the expression of an AP1μ2-RNAi construct under the control of the INNER NO OUTER (INO) promoter (INOpro:AP1μ2-RNAi) (Wang et al., 2016b). Although INOpro:AP1μ2-RNAi was previously reported to specifically downregulate the levels of AP1μ2 mRNA in the outer integuments of developing ovules (Wang et al., 2016b), we identified two independent INOpro:AP1μ2-RNAi transgenic lines (AP1μ2-RNAi-1 and AP1μ2-RNAi-2) that showed a ∼60% reduction in the expression of AP1μ2 mRNA relative to WT (Supplemental Figure S4, A). Although not as severe as homozygous ap1μ2 and ap1σ1 ap1σ2 double mutants, the AP1μ2-RNAi-1 and AP1μ2-RNAi-2 lines displayed defects in root growth (Park et al., 2013; Teh et al., 2013; Wang et al., 2013a; Supplemental Figure S4, B and C). Nevertheless, similar to homozygous ap1μ2 and ap1σ1 ap1σ2 double mutants, downregulation of AP1μ2 mRNA levels resulted in a significant loss of TGN/EE-associated GFP-tagged CLC3 and CHC2 in root cells (Supplemental Figures S4, D–G). In addition to the reduction in TGN/EE-associated clathrin, we also observed a loss of CHC and CLC isoforms at the PM in ap-1 mutants (Figure 1, A–D and Supplemental Figures S3, A–O, S4, D–G). Further analyses of the effects of loss of AP-1 on CME are described below.

Loss of AP-1 causes differential perturbation of TGN/EE-resident protein localization

The loss of TGN/EE-associated clathrin suggests that TGN/EE organization and/or function may be altered in ap-1 mutants. In agreement, the ultrastructure of the Golgi apparatus was previously shown to be altered in ap1μ2 mutant cells (Park et al., 2013). Therefore, to further probe the integrity of the Golgi apparatus in ap-1 mutants, we investigated the localization of the TGN/EE-resident proteins vacuolar ATPase subunit a1 (VHAa1), SYNTAXIN 41 (SYP41) and SYP61, which are required for post-Golgi trafficking, tagged with the fluorescent proteins RFP (VHAa1-RFP), GFP (SYP41-GFP), and cyan fluorescent protein (CFP-SYP61) (Uemura et al., 2004; Dettmer et al., 2006; Robert et al., 2008; Drakakaki et al., 2012). Live-cell imaging revealed that absence of AP1μ2 does not change the signal intensity or density of TGN/EE labeled by VHAa1-RFP (Figure 2, A–D). By contrast, we observed the mislocalization of SYP41-GFP and SYP61-CFP to the PM, as well as a significant decrease in the fluorescence signal intensity and density of TGN/EE-associated SYP41-GFP and SYP61-CFP in ap1μ2 root cells relative to wild-type (WT) root cells (Figure 2, H–K, O–R).
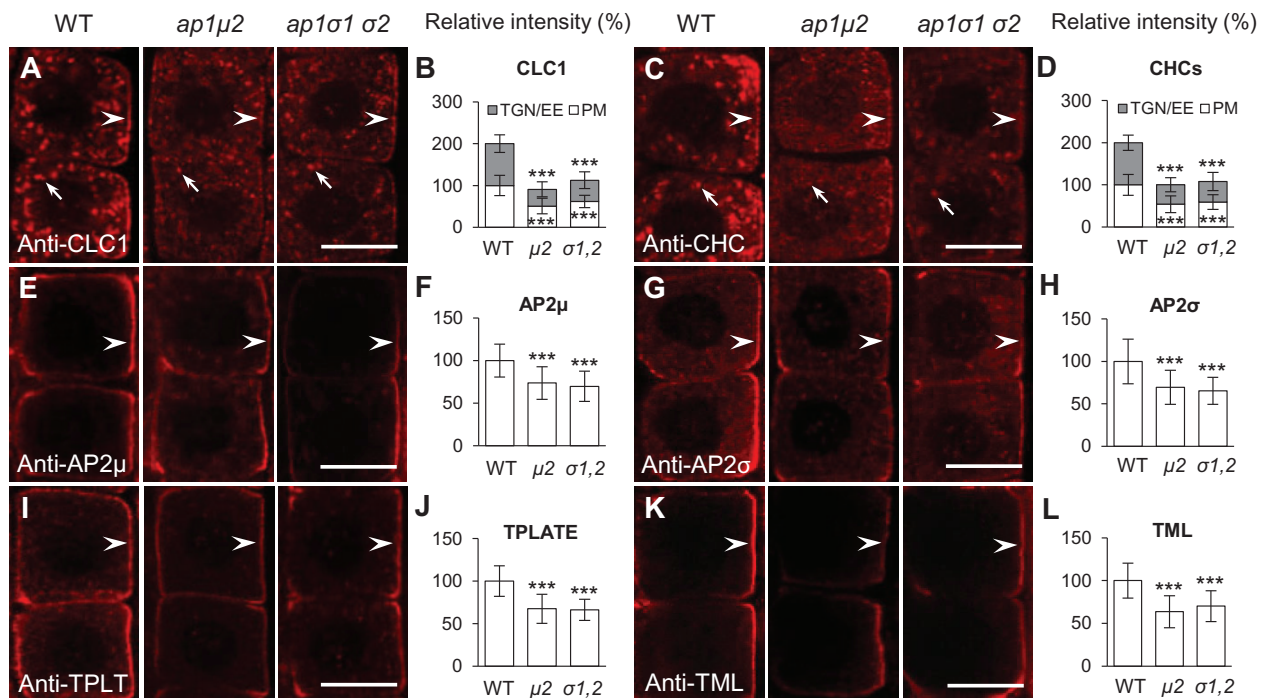
Figure 1 Levels of membrane-associated clathrin, AP-2, and TPC are reduced in *ap-1* mutant root cells. A–L, IF microscopy of PM- and/or TGN/EE-associated CLC1 (A, B), CHCs (C, D), AP2μ (E, F), AP2σ (G, H), TPLATE (I, J), and TPLATE-like (TML; K, L) in the WT Col-0 and *ap-1*. B, D, F, H, J, and L, Quantitative analysis of the relative intensities of CLC1, CHCs, AP2μ, AP2σ, TPLATE, and TML at the PM and/or TGN/EE (B, $n = 70–105$ cells from 8 to 10 roots each; D, $n = 58–84$ cells from 8 to 11 roots each; F, $n = 74–103$ cells from 6 to 15 roots each; H, $n = 66–150$ cells from 7 to 22 roots each; J, $n = 78–114$ cells from 7 to 13 roots each; L, $n = 54–72$ cells from 7 to 8 roots each). Arrows show representative clathrin-associated TGN/EE. Arrowheads show representative regions of the PM containing clathrin, AP-2, or TPC subunits, respectively. Shown are means ± SD. ***$P < 0.0001$ (Student's *t* test; compared with the WT). Bars = 10 μm.

Moreover, treatment of *ap1μ2* mutants with the vesicle trafficking inhibitor brefeldin A (BFA), which causes aggregation of TGN/EE membranes in plant cells (Geldner et al., 2003; Lam et al., 2009), resulted in differential accumulation of VHAa1-RFP, SYP41-GFP, and SYP61-CFP in BFA bodies. While we observed no detectable differences in the formation of BFA bodies containing VHAa1-RFP in WT or *ap1μ2* mutant root cells treated with 50 μM BFA for 10 min (Figure 2, E–G), we did notice a significant reduction in the size of SYP41-GFP and SYP61-CFP labeled BFA bodies in *ap1μ2* mutant cells relative to WT (Figure 2, L–N, S–U). These results demonstrate that localization of the TGN/EE-resident proteins SYP41 and SYP61, but not that of VHAa1, is affected in *ap1μ2* mutants, suggesting that loss of AP-1 has differential effects on the localization of TGN/EE-resident proteins and/or the organization of this compartment.

Disruption of clathrin or AP-1 impairs post-Golgi trafficking to the PM

The TGN/EE is involved in post-Golgi trafficking of soluble and membrane cargoes to the vacuole and PM (Lam et al., 2007; Gendre et al., 2015). To address whether the loss of TGN/EE-associated clathrin or AP-1 affected exocytosis, we assessed the intracellular trafficking and delivery of the soluble secreted marker sec-GFP (Zheng et al., 2004) to the apoplast in the root cells of mutants defective for subunits of

clathrin or the AP-1 complex. Consistent with the secretion defects previously observed in *chc1-2* and *chc1-3* (Larson et al., 2017) and *ap1μ2* mutants (Park et al., 2013), sec-GFP accumulated within intracellular compartments in *chc1*, *chc2*, *chc1/CHC1 chc2*, and *clc2 clc3* mutants as well as in *ap1μ2* and *ap1σ1-1 ap1σ2-1* double mutants (Figure 3, A–C, F–L). Notably, the levels of intracellular sec-GFP fluorescence signal in mutants defective for clathrin or AP-1 subunits were similar to those observed in WT seedlings treated with endosidin 2 (ES2), an inhibitor of exocytosis (Zhang et al., 2016; Figure 3, D–F).

We previously showed that clathrin is necessary for the recycling of internalized PM proteins to the PM (Wang et al., 2013b). Therefore, we examined whether AP-1 was required for the recycling of the PM marker proteins auxin efflux transporter PIN-FORMED 2 (PIN2-GFP) and RARE COLD-INDUCIBLE 2A (RCI2A-GFP). To monitor recycling, WT and mutant root cells expressing *PIN2-GFP* or *RCI2A-GFP* were treated for 60 min with the reversible trafficking inhibitor BFA, in the presence of the protein synthesis inhibitor cycloheximide (CHX) to entrap the PM internalized marker proteins in BFA bodies. Following BFA washout, we analyzed the loss of BFA body-associated PIN2-GFP or RCI2A-GFP by confocal microscopy and quantitative image analysis. As shown in Supplemental Figure S5, recycling to the PM of PIN2-GFP and RCI2A-GFP was reduced in the
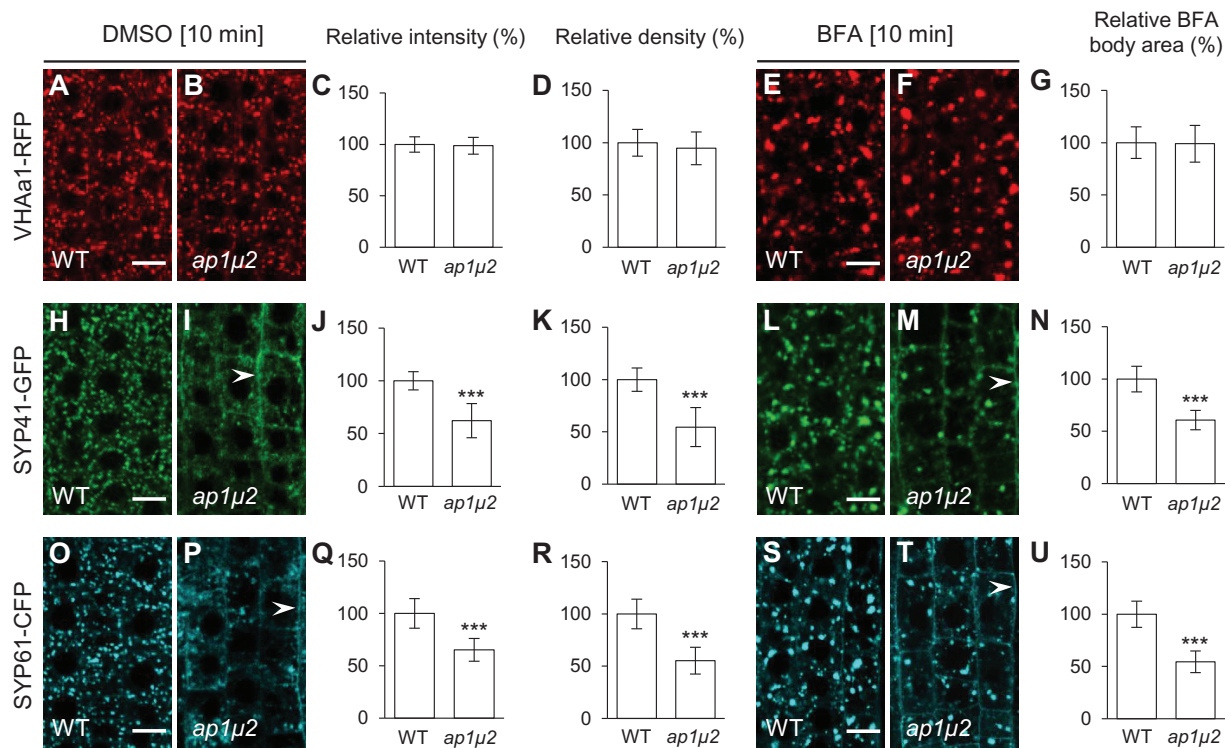
Figure 2 Localization of the TGN/EE-resident proteins, SYP41 and SYP61 but not VHAa1 is affected in *ap-1* mutants. A–D, H–K, and O–R, Confocal microscopy imaging of the subcellular distribution of TGN/EE markers, VHAa1-RFP (A–D), SYP41-GFP (H–K), and SYP61-CFP (O–R) in WT and *ap-1* mock-treated with DMSO for 10 min. C, J, and Q, Relative fluorescent signal intensities of VHAa1-RFP, SYP41-GFP, and SYP61-CFP at the TGN/EE (C, n = 98–122 cells from 10 to 15 roots each; J, n = 107–141 cells from 11 to 14 roots each; Q, n = 102–154 cells from 10 to 16 roots each). D, K, and R, Relative density of VHAa1-RFP-, SYP41-GFP-, and SYP61-CFP-labeled TGN/EE bodies per area of a cell (D, n = 98–122 cells from 10 to 15 roots each; K, n = 107–141 cells from 11 to 14 roots each; R, n = 102–154 cells from 10 to 16 roots each). E–G, L–N, and S–U, VHAa1-RFP (E–G), SYP41-GFP (L–N), and SYP61-CFP (S–U) in the WT and *ap-1* roots treated with BFA for 10 min. G, N, and U, Relative VHAa1-RFP-, SYP41-GFP-, and SYP61-CFP-labeled BFA body areas (G, n = 110–163 cells from 10 to 12 roots each; N, n = 97–138 cells from 9 to 13 roots each; U, n = 104–156 cells from 9 to 12 roots each). Arrowheads in (I), (M), (P), and (T) show mislocalization of SYP41-GFP and SYP61-CFP to the PM in the *ap-1* mutant relative to WT root cells. Shown are means ± SD. ***P < 0.0001 (Student's *t* test; compared with the WT). Bars = 10 μm.

ap1μ2 and *ap1σ1-1 ap1σ2-1* mutants, relative to the WT. These results together suggest that clathrin and AP-1 are necessary for exocytic trafficking of secreted and recycling of endocytosed proteins to the PM.

Defects in AP-1 affect endocytosis

In addition to defects in secretion, *ap1μ2* mutants have also been reported to exhibit delayed internalization of the lipophilic PM tracer dye FM4-64 (Teh et al., 2013), suggesting that AP-1 is required for endocytosis. However, other studies have reported contradictory results, including no significant defects in internalization (Park et al., 2013) and increased FM dye internalization (Wang et al., 2013a) in *ap1μ2* mutants versus WT. Therefore, we sought to reevaluate whether AP-1 function is necessary for endocytosis of FM4-64.

To assess FM4-64 uptake in WT and *ap-1*-mutant cells, we initially loaded the dye into the PM of seedling root cells under low temperature conditions (4 °C), which inhibit CME (Bolte et al., 2004; Dhonukshe et al., 2007). Prior to shifting the cells to 23 °C, the initial FM4-64 fluorescence signal intensity was identical at the PM of WT, *ap1μ2*, and *ap1σ1-1 ap1σ2-1* root epidermal cells, with no detectable

intracellular accumulation of the dye (Figure 4, A and B). Following a 6-min incubation at 23 °C during which CME is active, intracellular FM4-64-labeled puncta became readily apparent in WT root cells (Figure 4, C and D). By contrast, the ratio of intracellular/PM FM4-64 signal was significantly lower in *ap1μ2*, and *ap1σ1-1 ap1σ2-1* mutant root cells relative to WT (Figure 4, C and D). Internalized FM4-64 in both WT and *ap1μ2* root cells predominantly colocalized with CLC2-GFP (Supplemental Figure S6), suggesting that loss of AP-1 function reduces FM4-64 endocytosis, but not its delivery to the TGN/EE. Similarly, partial downregulation of *AP1μ2* through use of the *AP1μ2*-RNAi-1 and *AP1μ2*-RNAi-2 lines resulted in a reduction of FM4-64 internalization relative to WT, although not as severely as in *ap1μ2*-mutant lines (Supplemental Figure S4, H–K).

Disruption of AP-1 or exocytosis affected clathrin and CME accessory protein localization to the PM

Consistent with the reduction in FM4-64 internalization seen in *ap-1* mutants (Figure 4, A–D and Supplemental Figure S4, H–K), loss of AP-1 function resulted in a decrease in the levels of CHC and CLC isoforms at the PM (Figure 1, A–D and
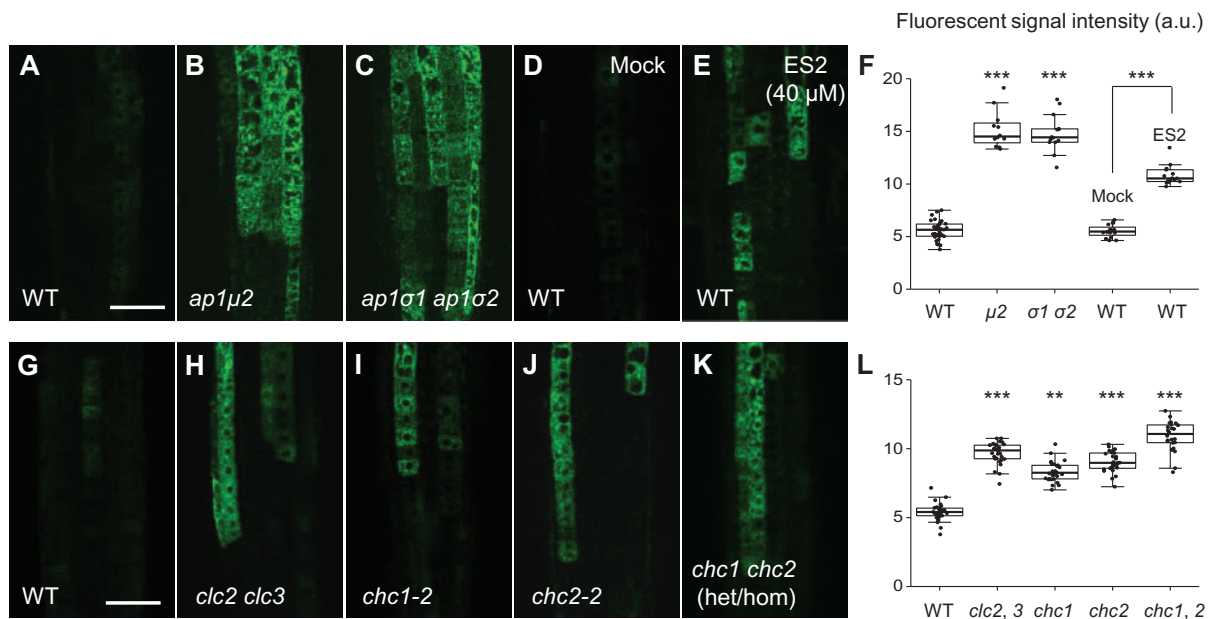
Figure 3 Impaired secretion of Sec-GFP in *ap-1*, *clc*, *chc* mutants and ES2-treated roots. A–F, Sec-GFP secretion in WT (A) and *ap-1* (B, C) roots or in WT roots mock-treated (DMSO; D) or treated with ES2 (E) for 4 h. G–L, Sec-GFP secretion in the WT (G) and *clc2 clc3* double mutant (H), *chc1-2* mutant (I), *chc2-2* mutant (J), and *chc1/CHC1 chc2* mutant (K) roots. F and L, Boxplot representation of Sec-GFP fluorescent signal intensities (in arbitrary units, a.u.) in the roots (F, *n* = 32, 12, 14, 16, and 15 measurements, respectively; L, *n* = 30, 29, 30, 27, and 24 measurements, respectively). Each data point represents an individual root. **$P < 0.001$, ***$P < 0.0001$ (Student's *t* test; compared with the WT or the mock). Bars = 50 μm.

Supplemental Figures S3, A–O, S4, D–G). Therefore, we examined whether the PM localization of endocytosis accessory proteins was also affected in loss-of-function *ap-1* mutants by quantitative IF microscopy. Accordingly, we conducted immunolocalization using affinity-purified anti-AP2μ, anti-AP2σ (Wang et al., 2016a), anti-TPLATE, and anti-TML antibodies (see Methods and Supplemental Table S2 for description of antibodies). The specificity of anti-TPLATE/TML antibodies was confirmed by IF analysis (Supplemental Figure S7, A) on seedling roots in which the levels of *TPLATE* and *TML* mRNA were lowered through expression of the estradiol-inducible artificial microRNA (amiR) constructs amiR-*TPLATE* and amiR-*TML* (Gadeyne et al., 2014; Wang et al., 2016a). Consistent with the reduced endocytic internalization of FM4-64 in *ap-1* mutants (Figure 4, A–D), the levels of PM-associated AP-2 (AP2μ and AP2σ) and TPC (TPLATE and TML) were reduced in *ap1μ2* single and *ap1σ1 ap1σ2* double mutants by ~25%–30% and ~25%–40%, respectively, relative to WT (Figure 1, E–L). Similarly, PM-associated levels of the transgenically derived DYNAMIN-RELATED PROTEIN1 (DRP1) family members DRP1A-GFP and DRP1C-GFP, which are required for CME (Konopka et al., 2008; Fujimoto et al., 2010), were also reduced in *ap1μ2* (Supplemental Figure S8, A–F).

To further examine how loss of AP-1 affects the PM localization of clathrin and endocytic accessory proteins, we utilized total internal reflection fluorescence (TIRF) microscopy to analyze the membrane association and lifetime of PM-associated CLC3-GFP, AP2μ-YFP, and TML-YFP in WT and *ap1μ2* root epidermal cells. In agreement with the observed reduction in overall levels of clathrin and endocytic accessory

factors at the PM (Figure 1 and Supplemental Figures S3, A–O, S4, D–G, L–O), the densities of foci containing CLC3-GFP (Figure 5, A and B; regular/small foci; ~46% reduction), AP2μ-YFP (Figure 5, C and D; ~38% reduction), and TML-YFP (Figure 5, E and F; ~51% reduction) were visibly reduced in the *ap1μ2* mutant relative to the WT. However, the frequency distribution and average lifetime of PM-associated CLC3-GFP, AP2μ-YFP, and TML-YFP foci in *ap1μ2* were similar to the WT (Figure 5, G–O and Supplemental Movies S1–S3). The number of CLC3-GFP-labeled TGN/EE, which appear as large bright structures when they enter the cortical TIRF imaging field (Supplemental Movie S1), was also significantly reduced (Figure 5, A and B; large structure), likely due to the decreased levels of TGN/EE-associated clathrin in the *ap1μ2* mutant relative to WT cells (Figure 1, A–D and Supplemental Figures S3, A–O, S4, D–G).

We corroborated the reduction in the levels of membrane-associated clathrin and clathrin-associated factors in *ap1μ2* relative to WT seedlings by quantitative immunoblot analysis. We detected no significant differences in the abundance of CLC1-3, CHC1-2, AP2μ, or AP2σ in total protein extracts from *ap1μ2* and WT seedlings (Figure 6). Likewise, the levels of TPLATE, TML, DRP1A, and DRP1C were similar in protein lysates from WT and *ap1μ2* seedlings accumulating GFP/YFP-tagged fusions of these proteins (Figure 6 and Supplemental Figure S8, G–I). The specificity of the anti-GFP antibody is shown in Supplemental Figure S7, B. Loss of AP1μ2, however, resulted in a decrease in microsomal membrane-associated clathrin and clathrin accessory proteins, with a corresponding increase in the levels of
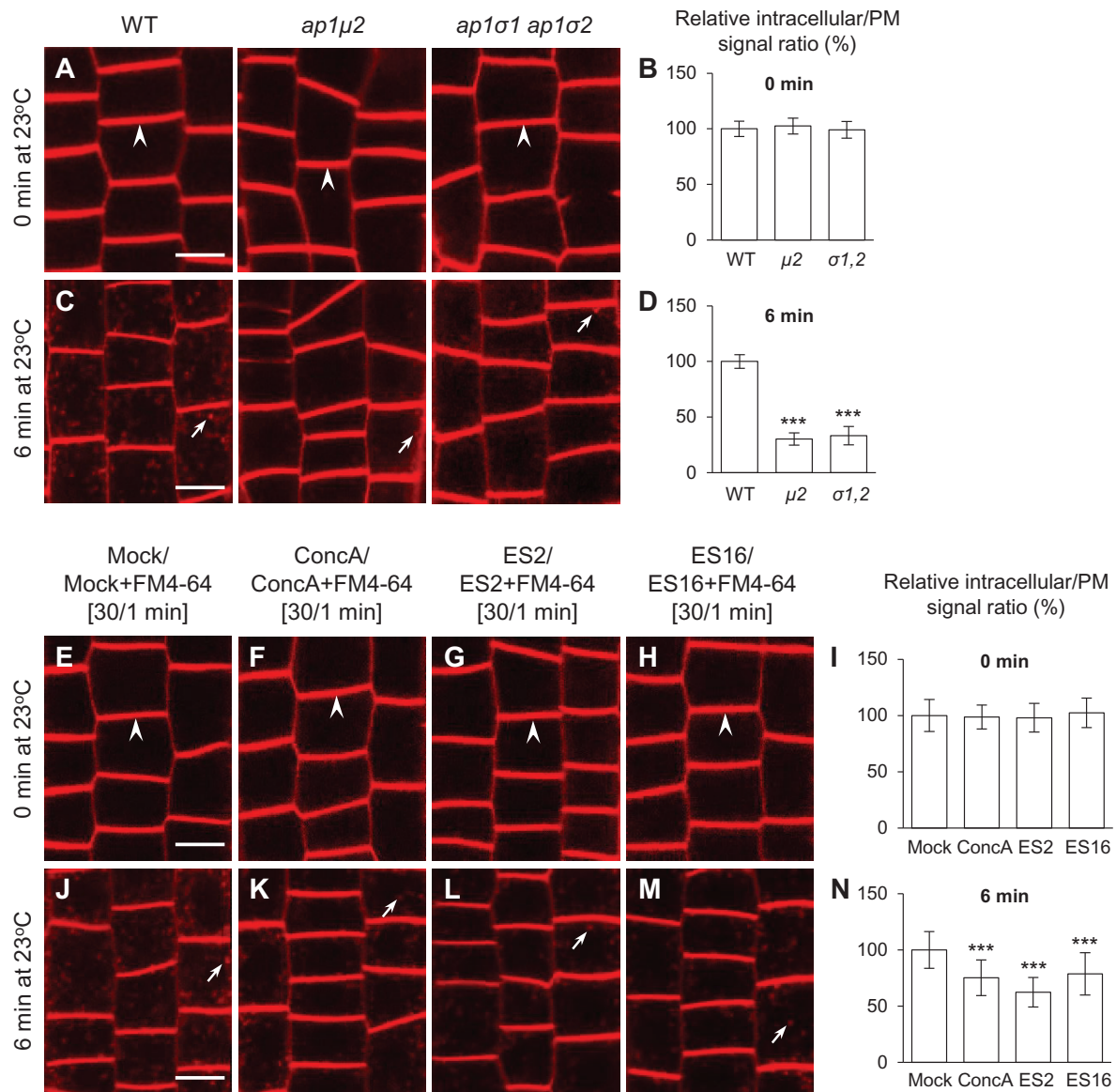
Figure 4 AP-1 disruption or exocytosis/PM recycling inhibitors impair FM4-64 internalization in root cells. A–D, Confocal microscopy analysis of FM4-64 internalization in WT and *ap-1* meristem epidermal root cells. Seedling roots were labeled with dye for 1 min on ice and either directly imaged (0 min) or after 6 min incubation at 23 °C. B, D, Quantitative analysis of the relative ratios of the intracellular to PM fluorescent signal of FM4-64 labeled WT and *ap-1* mutant root cells after incubation for 0 or 6 min at 23 °C (B, $n = 158$–264 cells from 7 to 12 roots each; D, $n = 129$–178 cells from 13 to 18 roots each). E–N, FM4-64 uptake in WT roots either mock-treated (DMSO) or treated with ConcA, ES2, and ES16, respectively. I and N, Quantitative analysis of the relative ratios of the intracellular to PM fluorescent signal of FM4-64-labeled WT root cells after incubation for 0 or 6 min at 23 °C (I, $n = 203$–267 cells from 12 to 14 roots each; N, $n = 226$–281 cells from 12 to 15 roots each). The seedlings were pretreated with DMSO or exocytic inhibitors for 30 min, followed by labeling with DMSO/exocytic inhibitors and FM4-64 for 1 min on ice before immediate or delayed imaging. Arrows and arrowheads show representative FM4-64-labeled vesicles or PM-bound FM4-64, respectively. Shown are means ± SD. ***$P < 0.0001$ (Student's *t* test; compared with the WT or the mock). Bars = 10 μm.

these proteins in the soluble protein fraction (Figure 6 and Supplemental Figure S8, G–I). We used the fractionation of the integral endoplasmic reticulum membrane marker protein sterol methyltransferase1 (SMT1) (Boutté et al., 2010) as a control to assess the samples enriched in soluble and microsomal membrane proteins from WT and *ap1μ2* seedlings. As shown by immunoblot analysis using anti-SMT1 antibodies, SMT1 predominantly fractionated in the microsomal membrane-enriched protein samples from WT and

ap1μ2 seedlings (Supplemental Figure S7, C). Furthermore, RT-qPCR showed that loss of AP1μ2 does not alter the expression of genes encoding clathrin subunits or clathrin accessory factors (Supplemental Figure S9). Taken together, these results suggest that the reduction in the levels of PM- and TGN/EE-associated clathrin and its accessory proteins in *ap-1* mutants is likely due to defects in their membrane recruitment rather than changes in its expression levels and/ or its degradation.
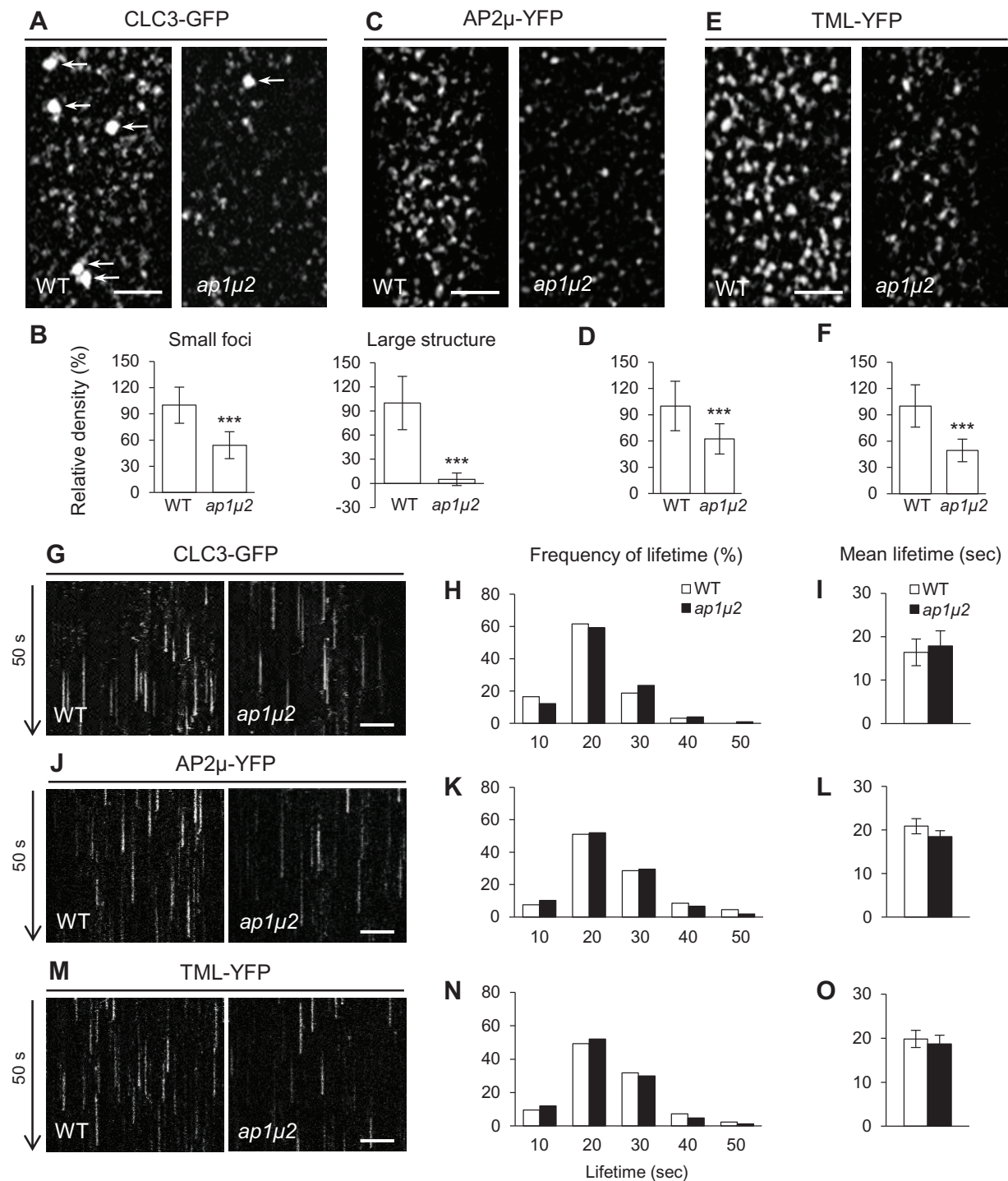
Figure 5 The density, but not the lifetime of PM-associated clathrin, AP-2, and TPC foci is reduced in *ap-1* mutants. A–F, TIRF microscopy analysis of PM-associated foci of CLC3-GFP (A, B), AP2μ-YFP (C, D), and TML-YFP (E, F) in WT and *ap1μ2*. B, D, and F, Relative densities of PM-associated foci (B, left/small foci, *n* = 63–85 cells from 14 to 23 roots each; right/large structure, *n* = 46–50 cells from 14 to 23 roots each; D, *n* = 112–183 cells from 22 to 46 roots each; F, *n* = 93–101 cells from 25 to 36 roots each). G, J, and M, Kymographs of PM-associated foci in WT and *ap1μ2*. H, K, and N, Frequency distribution of lifetimes for PM-associated foci in WT and *ap1μ2*. I, L, and O, Mean lifetimes of PM-associated foci in WT and *ap1μ2* (H and I, *n* = 1,860–2,022 foci from 12 to 13 roots each; K and L, *n* = 1,738–1,821 foci from 10 to 12 roots each; N and O, *n* = 1,668–1,894 foci from 11 to 13 roots each). White and black arrows indicate CLC3-GFP-labeled TGN/EE and time direction, respectively. Shown are means ± SD. ***$P < 0.0001$ (Student's *t* test; compared with the WT). Bars = 5 (A, C, and E) or 2 μm (G, J, and M).
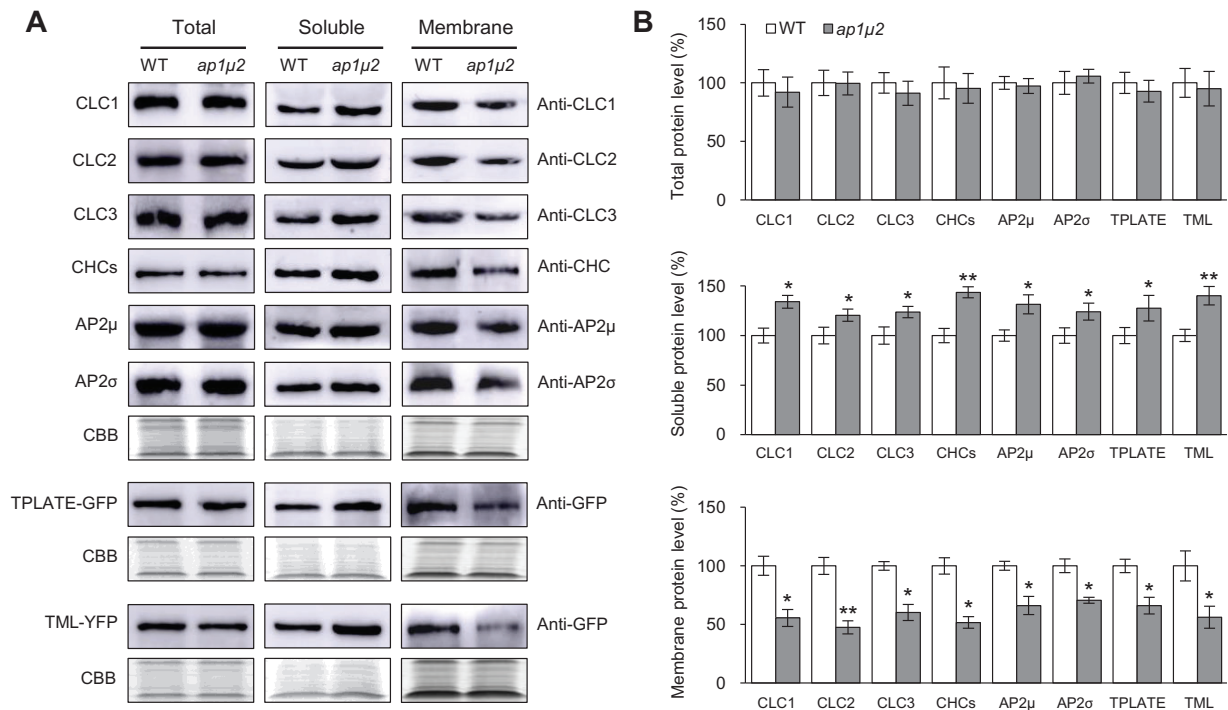
Figure 6 Membrane recruitment of clathrin, AP-2, and TPC is reduced in *ap-1* mutant seedlings. A, Immunoblot analysis of the levels of clathrin, AP-2, and TPC in total, soluble, and membrane-enriched protein extracts from 5-day-old WT and *ap1μ2* seedlings. B, Quantitative analysis of the immunoblot signal intensities in (A). Average immunoblot signal intensity was derived from three independent experiments. CBB staining served as a loading control. Shown are means ± SD. *$P < 0.05$; **$P < 0.001$ (Student's *t* test; compared with the WT).

Pharmacological inhibitors of exocytosis cause defects in endocytosis and the recruitment of CME proteins to the PM

The results described above indicate that both exocytosis and endocytosis are impaired in *ap-1* mutants, suggesting that these trafficking pathways are interconnected. To further investigate whether CME is more broadly dependent on exocytosis, we examined the effects of inhibitors that block post-Golgi/endosomal and exocytic trafficking on CME in plant cells. However, in contrast to *ap-1* mutants that displayed altered TGN/EE-resident protein localization (Figure 2), there was no discernable difference between the subcellular distribution or fluorescence signal intensity of TGN/EE-associated VHAa1-RFP, SYP41-GFP, and SYP61-CFP in seedling root cells treated for 1 h with concanamycin A (ConcA; Gendre et al., 2011), ES2 (Zhang et al., 2016), or ES16 (Li et al., 2017), relative to mock controls (Supplemental Figure S10). Nevertheless, similar to mutants defective in AP-1 function, the internalization of FM4-64 in WT root cells treated with ConcA, ES2, or ES16 significantly decreased compared with the mock control (Figure 4, E–N).

Impaired internalization of FM4-64 with ConcA, ES2, and ES16 was associated with a decrease in the levels of clathrin at TGN/EE and PM as well as a reduction in clathrin accessory proteins at the PM (Supplemental Figures S11, S12). In root cells of WT seedlings treated with ConcA (5 μM), ES2 (40 μM), or ES16 (20 μM) for 60 min, we observed a reduction in the levels of PM-associated AP2μ-YFP/AP2σ-GFP and TPLATE-GFP/TML-YFP (Supplemental Figure S12) as

well as the loss of PM- and TGN/EE-associated CLC3-/CHC2-GFP (Supplemental Figure S11), relative to the mock control. These results are supported by quantitative immunoblot analysis confirming that the levels of membrane-associated clathrin and AP-2/TPC, as well as DRP1A and DRP1C, are reduced in seedlings treated with inhibitors of exocytosis/PM recycling relative to the mock control (Supplemental Figure S13). Together, these data support a model wherein inhibition of exocytic trafficking due to the loss of AP-1 function or treatment with small molecule inhibitors of exocytosis causes impaired CME.

Inhibition of CME impairs exocytosis

To address the reciprocal question of whether inhibition of CME affects post-Golgi trafficking, we examined trafficking of PIN2-GFP and RCI2A-GFP from BFA bodies in root epidermal cells lacking AP-2 or TPC subunits. Previous studies have shown that PIN2-GFP and RCI2A-GFP recycling from the TGN/EE to the PM is dependent on clathrin function (Kitakura et al., 2011; Wang et al., 2013b). Similarly, the trafficking of internalized PIN2-GFP (Figure 7, A–D) and RCI2A-GFP (Supplemental Figure S14, A–D) from BFA bodies following BFA removal in AP-2-deficient lines, *ap2μ-1* (Wang et al., 2016a) and *ap2σ-1* (Fan et al., 2013) was slower than that of WT. Likewise, estradiol-induced downregulation of *TPLATE* and *TML* transcript levels in amiR-*TPLATE* and amiR-*TML* lines (Gadeyne et al., 2014) resulted in inhibited recycling of internalized PIN2-GFP (Figure 7, E–H) and RCI2A-GFP (Supplemental Figure S14, E–H) to the PM.
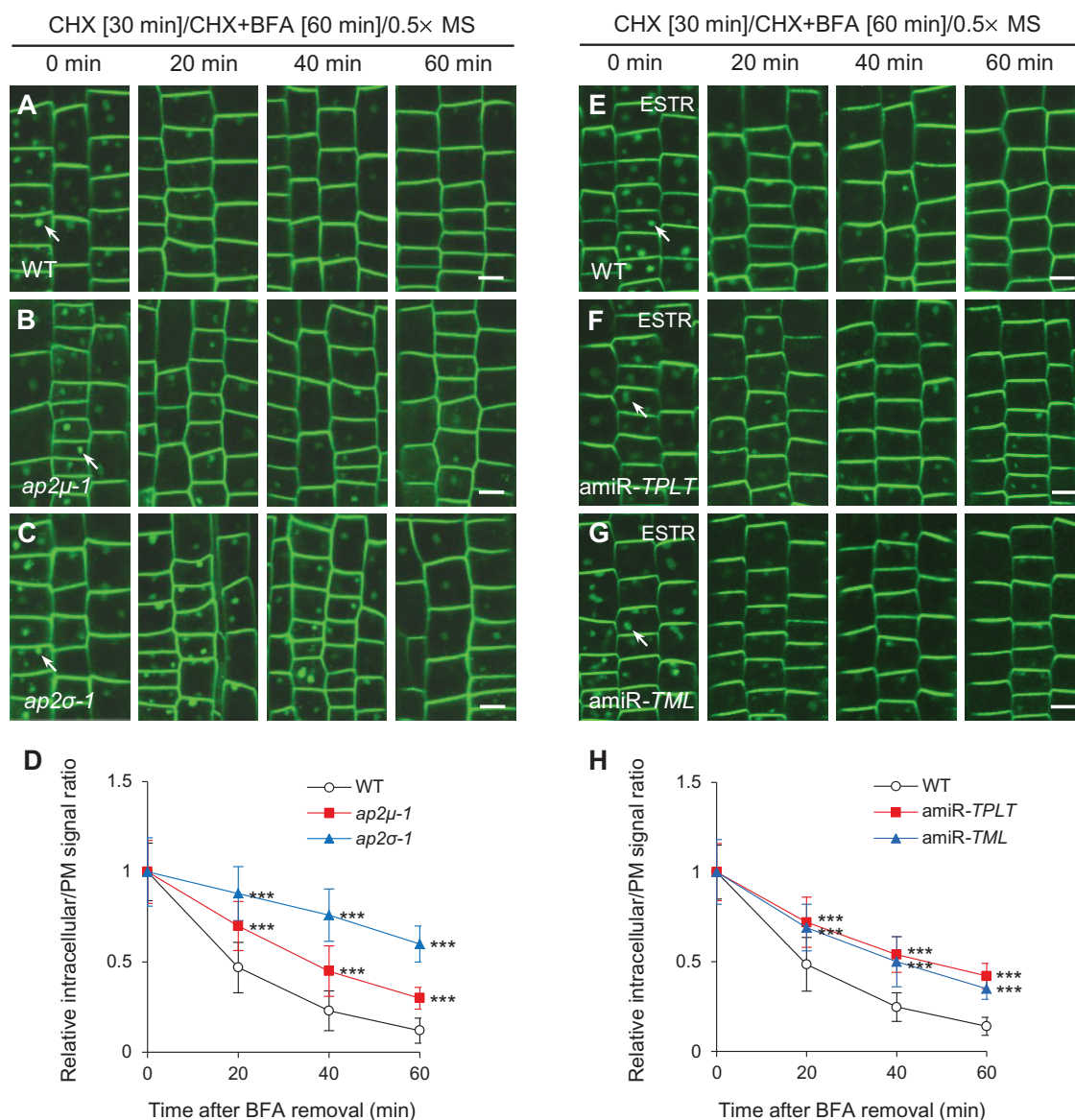
Figure 7 Recycling of endocytosed PIN2-GFP from BFA bodies to the PM is reduced in *ap-2* and *tpc* mutants. A–H, Recycling of internalized PIN2-GFP from BFA bodies to the PM in WT, *ap-2*, and *tpc* root meristem epidermal cells following BFA washout. D and H, Quantification of the relative ratios of intracellular to PM fluorescent signals after BFA removal in WT (D, $n = 532$–681 cells from 17 to 19 roots each; H, $n = 564$–736 cells from 13 to 15 roots each), *ap-2* (D, $n = 498$–664 cells from 16 or 17 roots each in *ap2μ-1*; $n = 357$–416 cells from 10 to 12 roots each in *ap2σ-1*), and *tpc* (H, $n = 694$–757 cells from 13 to 15 roots each in amiR-*TPLATE*; $n = 672$–785 cells from 14 to 15 roots each in amiR-*TML*). ESTR, estradiol. The seedlings were pretreated with CHX for 30 min, followed by addition of CHX and BFA for 60 min, prior to washout of the inhibitors with liquid half-strength MS medium for different lengths of time (0, 20, 40, and 60 min) prior to confocal imaging. Arrows indicate representative BFA bodies containing endocytosed PIN2-GFP. Shown are means ± SD. ***$P < 0.0001$ (Student's *t* test; compared with the WT). Bars = 10 μm.

In addition to affecting PM protein recycling, inhibition of CME reduced the secretion of de novo-synthesized proteins. Analysis of *ap-2* mutants (*ap2μ-1* and *ap2σ-1*; Figure 8, A–D) as well as of TPC-deficient lines (amiR-*TPLATE* and amiR-*TML* in the presence of 20 μM estradiol; Figure 8, G–K), accumulating the secretory reporter sec-GFP, showed a marked increase in intracellular GFP fluorescence relative to the WT control and the mock control (Figure 8, A, G, and I), respectively. Sec-GFP secretion was not affected in WT cells treated with estradiol (20 μM; Figure 8, F), indicating that the observed inhibition of sec-GFP trafficking in the

amiR-*TPLATE* and amiR-*TML* lines is specific to the inhibition of *TPLATE* and *TML* transcript levels.

Interference of CME impairs AP-1 recruitment to the TGN/EE

As shown previously, defects in the endocytic adaptor complexes AP-2 or TPC result in the loss of PM- and TGN/EE-associated clathrin (Wang et al., 2016a). To examine if AP-2 or TPC functions are likewise required for AP-1 recruitment to the TGN/EE, we analyzed the association of fluorescent protein-tagged AP1μ2 (AP1μ2-RFP) and AP1σ2 subunits
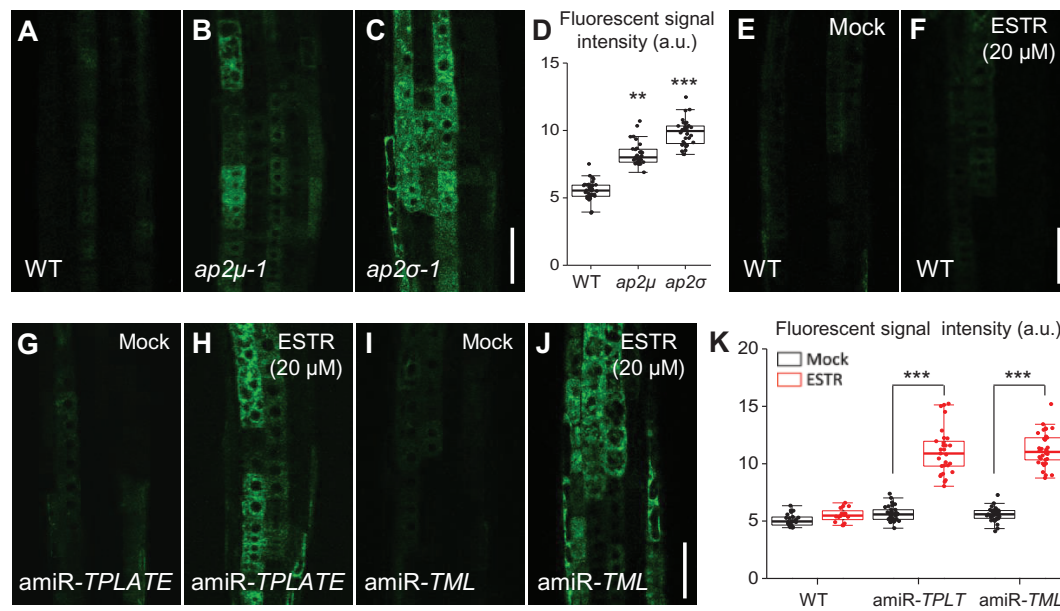
Figure 8 Secretion of Sec-GFP is impaired in *ap-2* and *tpc* mutants. A–K, Localization of sec-GFP secretion in WT (A, E, and F), *ap-2* (B and C), and *tpc* (G–J) roots. E and F, Localization of sec-GFP in DMSO- (mock; E) or estradiol- (ESTR; F) treated WT roots. D and K, Boxplot representation of sec-GFP fluorescent signal intensities (in arbitrary units, a.u.) in the roots (D, $n = 36$, 32, and 33 measurements, respectively; K, $n = 23$, 16, 32, 29, 34, and 33 measurements, respectively). Each data point represents an individual root. **$P < 0.001$; ***$P < 0.0001$ (Student's *t* test; compared with the WT or the mock). Bars = 50 μm.
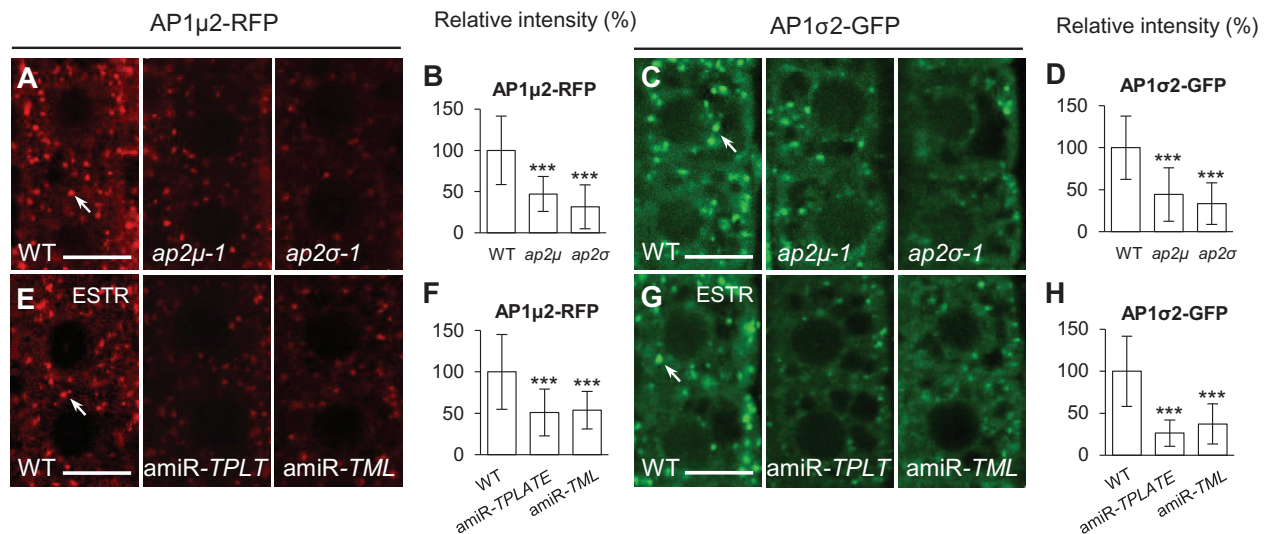

Figure 9 Loss of TGN/EE-associated AP-1 in *ap-2* and *tpc* mutants. A–H, Analysis of TGN/EE-associated AP1μ2-RFP and AP1σ2-GFP in WT, *ap-2*, and *tpc* root meristem epidermal cells. B, D, F, and H, Relative intensities of AP1μ2-RFP and AP1σ2-GFP at the TGN/EE (B, $n = 71$–77 cells from 9 to 11 roots each; D, $n = 88$–102 cells from 11 to 13 roots each; F, $n = 96$–104 cells from 12 to 13 roots each; H, $n = 88$–96 cells from 11 to 12 roots each). ESTR, estradiol. Arrows show representative AP1μ2-RFP- or AP1σ2-GFP-labeled TGN/EE. Shown are means ± SD. ***$P < 0.0001$ (Student's *t* test; compared with the WT). Bars = 10 μm.

(AP1σ2-GFP) with the TGN/EE in WT, *ap-2*, and *tpc* mutant lines (Figure 9). By live-cell imaging, we observed a reduction of TGN/EE-associated levels of AP1μ2-RFP and AP1σ2-GFP in loss-of-function *ap2μ-1* (∼53% and ∼56% reduction, respectively) and *ap2σ-1* (∼68% and ∼66% reduction, respectively) mutant lines relative to WT (Figure 9, A–D). Similarly, downregulation of *TPLATE* and *TML* transcript levels in estradiol-treated amiR-*TPLATE* and amiR-*TML* seedlings

(Gadeyne et al., 2014; Wang et al., 2016a) resulted in a loss of TGN/EE-associated AP1μ2-RFP (Figure 9, E and F) and AP1σ2-GFP (Figure 9, G and H) in seedling root cells following treatment for 5 days with 20 μM estradiol. RT-qPCR demonstrated that the reduction in levels of TGN/EE-associated clathrin and AP-1 subunits is not due to changes in transcript levels in *ap-2* and *tpc* mutants (Wang et al., 2016a; Supplemental Figure S15, A and C).

To confirm that downregulation of the levels of TPLATE and TML is associated with the loss of TGN/EE-associated AP-1, we performed time course analyses of TPLATE and TML mRNA levels (Supplemental Figure S15, D) and TGN/EE localization of AP1μ2-RFP and AP1σ2-GFP (Supplemental Figure S16) following estradiol treatment of amiR-TPLATE and amiR-TML lines. Relative to mock (dimethyl sulfoxide, DMSO)-treated amiR-TPLATE and amiR-TML seedlings, there was a significant decrease in TPLATE and TML transcript levels after 8, 16, and 24 h of treatment with 20 μM estradiol (Supplemental Figure S15, D). Likewise, we observed a progressive depletion of TGN/EE-associated AP1μ2-RFP and AP1σ2-GFP in estradiol-treated amiR-TPLATE and amiR-TML seedling root cells over the same time course (Supplemental Figure S16, A). Immunoblot analysis of soluble- and membrane-enriched subcellular fractions confirmed that ap-2 loss of function mutants or downregulation of TPC subunit expression results in the loss of associated microsomal membranes and a corresponding increase in the levels of soluble CLC1 (Supplemental Figure S17, A and B), AP1μ2-RFP (Supplemental Figure S17, C and D), and AP1σ2-GFP (Supplemental Figure S17, E and F) relative to the WT. The specificity of the anti-RFP and anti-GFP antibodies for AP1μ2-RFP and AP1σ2-GFP, respectively, is shown in Supplemental Figure S7, B. By contrast, defects in AP-2 or TPC subunits did not alter the TGN/EE localization of the TGN/EE-resident marker proteins VHAa1-RFP, SYP41-GFP, or SYP61-CFP (Supplemental Figure S18).

To further explore the mechanism of how loss of AP-2/TPC subunits affects TGN/EE recruitment of clathrin and AP-1 subunits, we analyzed the dynamics of CLC3-GFP and AP1σ2-GFP association with the TGN/EE in the ap2σ-1 mutant and the amiR-TPLATE line using fluorescence recovery after photobleaching (FRAP; 60 and 120 min after photobleaching all fluorescence signals in cells of interest; for 5–6 cells/layer and 3–4 cell layers). The fluorescent signal recovery at the TGN/EE of CLC3-GFP and AP1σ2-GFP was much slower in ap2σ-1 or amiR-TPLATE than in the WT or the mock control (Figure 10). These results together suggest that loss of AP-2/TPC function impairs TGN/EE recruitment of clathrin and AP-1 subunits.

Discussion

Exocytosis and endocytosis are key to controlling the protein and lipid composition of the PM. Coupling between these trafficking pathways is therefore likely critical for the establishment and maintenance of signaling across the PM, as well as the activities of proteins involved in diverse processes at the cell surface, including nutrient uptake, cell wall biogenesis, and pathogen defense.

Rapid compensatory endocytosis in neurons and other animal cells that undergo large-scale regulated exocytosis has been well established (Watanabe et al., 2013; Houy et al., 2015; Gómez-Elías et al., 2020). Work in a variety of systems including yeast (Saccharomyces cerevisiae), Metazoa, Trypanosoma brucei, and plants has also suggested links between the machinery involved in constitutive exocytic

vesicle transport, docking, and fusion with the PM and CME (Riezman, 1985; Gurunathan et al., 2000; Sommer et al., 2005; Jose et al., 2015; Johansen et al., 2016; Boehm et al., 2017; Larson et al., 2017; Ravikumar et al., 2018). In Arabidopsis, mutants defective for exocytosis also display an inhibition of endocytosis, as observed in mutants lacking subunits of the STOMATAL CYTOKINESIS DEFECTIVE (SCD) complex, which are required for activation of post-Golgi vesicle-associated RabE1 GTPases, and in the secretory SNARE mutant syp121 (McMichael et al., 2013; Larson et al., 2017; Mayers et al., 2017). Likewise, loss of RabH1B, a Golgi-localized Rab GTPase that functions in the trafficking of CELLULOSE SYNTHASE 6 (CESA6) to the PM, affects both the exocytosis and endocytosis of CESA6 (He et al., 2018). In addition, the cytoskeleton has been demonstrated to function in the coordination of membrane transport to and from the PM (Stamnes, 2002; Meunier and Gutiérrez, 2016; Zhang et al., 2019). For example, RICE MORPHOLOGY DETERMINANT (RMD), an actin-organizing protein, is required for exocytic and endocytic trafficking necessary for root growth (Li et al., 2014). The results presented here and in the recent study by Larson et al. (2017) indicate that additional mechanisms involving the coordinated regulation of the recruitment of clathrin and its accessory factors to the PM and TGN/EE are important for modulating exocytic and endocytic membrane transport.

Clathrin and AP-1 are required for post-Golgi trafficking in plant cells

In mammalian cells, yeast, fungi, and Toxoplasma gondii, clathrin and AP-1 functions are necessary for post-Golgi trafficking from the TGN to endosomes and in the polarized trafficking of some PM proteins (Gall et al., 2002; Jaiswal et al., 2009; Pieperhoff et al., 2013; Castillon et al., 2018; Martzoukou et al., 2018; Casler et al., 2019; Gravotta et al., 2019). Similarly, in plant cells, post-Golgi exocytic and vacuolar protein trafficking are dependent upon clathrin and AP-1 (Song et al., 2006; Park et al., 2013; Teh et al., 2013; Wang et al., 2013a, 2013b; Larson et al., 2017; Shimizu et al., 2021; Figure 3 and Supplemental Figure S5). As shown in Figure 1 and Supplemental Figures S1, S3, AP-1 is required to recruit clathrin to the TGN/EE, which serves as a major hub for the sorting and trafficking of newly synthesized proteins and endocytic cargoes to the PM and vacuole.

However, it remains to be determined whether clathrin and AP-1 function directly in the formation of clathrin-coated transport vesicles at the TGN/EE for the delivery of proteins to the vacuole and/or PM in plant cells. Alternatively, clathrin and AP-1 may be required for the maintenance of TGN/EE structure and function (Pantazopoulou and Glick, 2019), and thus loss of either clathrin or AP-1 would result in general defects in biosynthetic and endocytic cargo sorting and trafficking to/from the TGN/EE. Our results revealed that loss of function of AP1μ2 results in the significant reduction of clathrin as well as AP1σ2 recruitment to the TGN/EE (Supplemental Figure
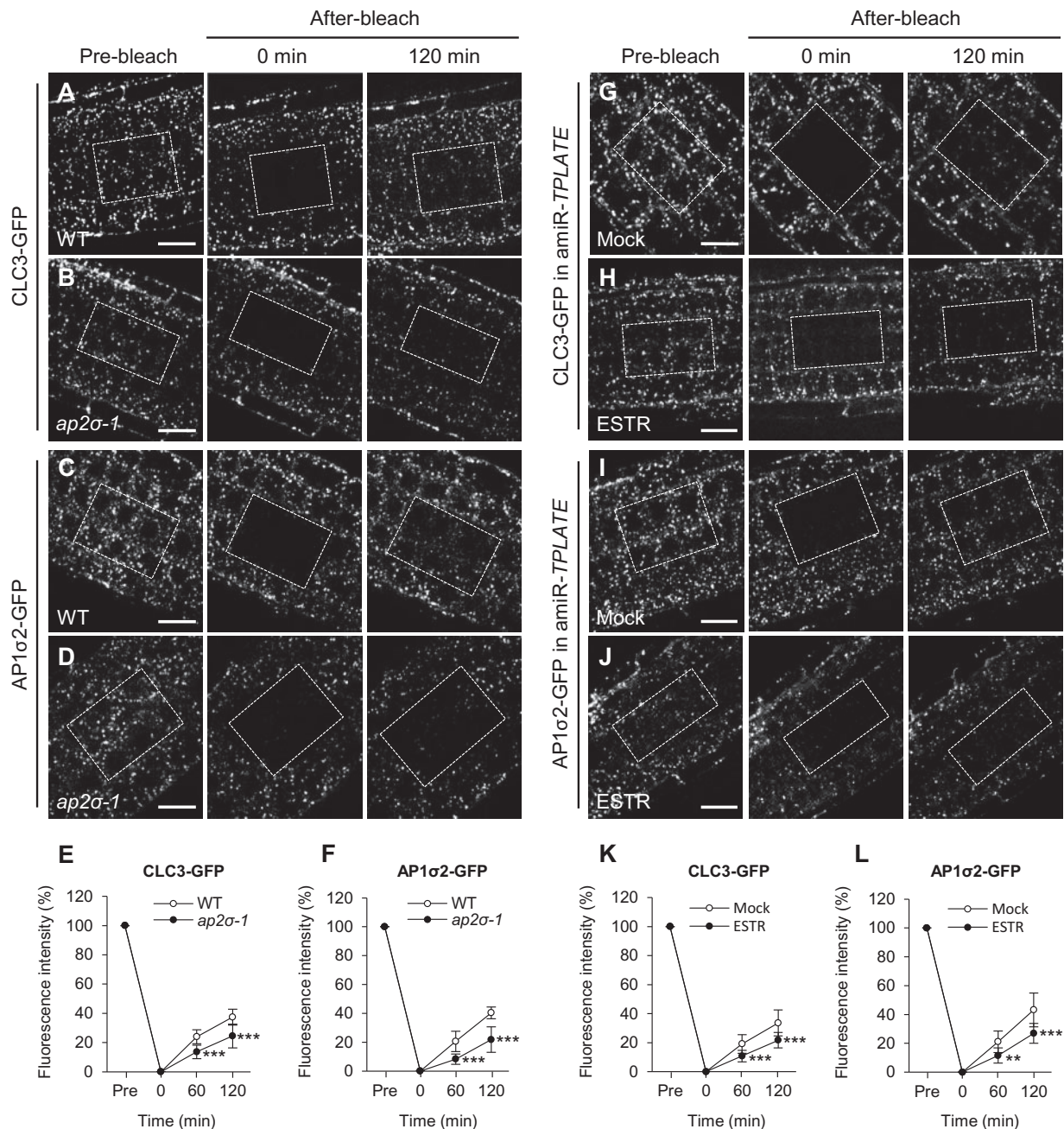
Figure 10 FRAP analysis of clathrin and AP-1 recruitment to the TGN/EE in *ap-2* and *tpc* mutants. A–F, TGN/EE recruitment of CLC3-GFP (A and B) and AP1σ2-GFP (C and D) in WT and *ap2σ-1*. E and F, Relative fluorescent signal intensities of TGN/EE-associated CLC3-GFP and AP1σ2-GFP (E, $n = 8$ roots each; F, $n = 7$ roots each). G–L, TGN/EE recruitment of CLC3-GFP (G and H) and AP1σ2-GFP (I and J) recruitment to the TGN/EE in amiR-*TPLATE* seedlings treated with DMSO (mock) or estradiol (ESTR). K and L, Relative fluorescent signal intensities of TGN/EE-associated CLC3-GFP and AP1σ2-GFP (K, $n = 9$ roots each; L, $n = 7$ roots each). Dashed boxes indicate bleached regions. Shown are means ± SD. **$P < 0.001$; ***$P < 0.0001$ (Student's *t* test; compared with the WT or the mock). Bars = 10 μm.

S3). Furthermore, *ap-1* mutants displayed differential changes in the localization/retention of TGN/EE-resident proteins (Figure 2). Taken together, these results provide further evidence of a relationship between clathrin- and AP-1-dependent protein trafficking and the integrity of the TGN/EE (Park et al., 2013; Wang et al., 2013a). Further studies are required to understand the molecular function of clathrin and AP-1 at the TGN/EE in plants. Nevertheless, our data demonstrate that disruption in post-Golgi trafficking due to

loss of TGN/EE-associated clathrin or AP-1 results in the inhibition of CME.

Coordinated regulation of exocytic and endocytic vesicle trafficking

Loss of AP-1 or treatment of WT seedlings with exocytosis inhibitors resulted in defects in the uptake of FM4-64 (Figure 4 and Supplemental Figure S4, H–K) and the membrane recruitment of clathrin and endocytic accessory

proteins (Figure 6 and Supplemental Figures S8, S13). However, disruption of AP-1 function and/or exocytosis did not alter the lifetimes of clathrin/AP-2/TPC foci on the PM (Figure 5 and Supplemental Movies S1–S3), suggesting that exocytosis modulates initiation but not the dynamics of CCV formation and budding during CME.

Similar to the manner in which defects in clathrin/AP-1-dependent post-Golgi trafficking negatively affect CME, disruption of CME in *ap-2* or *tpc* mutants was associated with a reduction in the levels of TGN/EE-associated clathrin and AP-1 subunits (Wang et al., 2016a; Figure 9 and Supplemental Figure S16) as well as impaired exocytic trafficking/secretion (Figures 7, 8). Collectively, these findings indicate that the association of clathrin and its accessory factors with the TGN/EE (AP-1/clathrin) and PM (AP-2/TPC/clathrin/DRP) is coordinately regulated, thereby coupling the processes of post-Golgi and endocytic trafficking in root cells. However, the signaling mechanisms by which clathrin-dependent exocytosis and CME are coupled remain to be identified.

The proper balance and maintenance of exocytosis and endocytic membrane transport is crucial for plant growth, development, and responses to various environmental cues (Zhang et al., 2019). During cytokinesis and cell expansion, the polarized delivery of endomembrane-derived vesicles to the cell plate and PM, respectively, is balanced by the retrieval of membrane and proteins (Samuels and Bisalputra, 1990; Otegui and Staehelin, 2000; Ketelaar et al., 2008). Discordance between exocytosis and endocytosis causes abnormal cell growth and morphogenesis in plants. For example, Arabidopsis *chc* mutants display defects in exocytosis and endocytosis and thereby develop aberrant cotyledons and embryos (Kitakura et al., 2011; Larson et al., 2017). Recent studies have also demonstrated that homeostasis of exocytosis and endocytosis is necessary for pollen tube tip growth, cold tolerance, stomatal movements, and osmotic stress response in plants (Deng et al., 2015; Zwiewka et al., 2015; Feng et al., 2016; Larson et al., 2017). The coupling of exocytosis and endocytosis may therefore be a critical point of regulation by developmental and environmental signals. Indeed, auxin and salicylic acid have been previously shown to rapidly (within 5 min of treatment) cause the dissociation of clathrin from both the TGN/EE and PM (Wang et al., 2013b, 2016a). However, the molecular mechanisms involved in the coordination of the recruitment of clathrin and its accessory factors to the PM and TGN/EE remain to be determined.

Materials and methods

Plant materials and growth conditions

The following transgenic lines and mutants were used in this study: transgenic lines *RPS5Apro:CHC1-GFP* (Dejonghe et al., 2016), *RPS5Apro:CHC2-GFP* (Ortiz-Morea et al., 2016), *35Spro:CLC1-GFP* (Wang et al., 2013b), *CLC2pro:CLC2-GFP* (Konopka et al., 2008), *CLC2pro:CLC2-mKO* (Ito et al., 2012), *CLC3pro:CLC3-GFP* (Dejonghe et al., 2016), *AP1μ2pro:AP1μ2-RFP* (Wang et al., 2013a), *35Spro:AP1σ2-GFP* (this study), *AP2μpro:AP2μ-YFP* (Bashline et al., 2013), *AP2σpro:AP2σ-GFP*

(Fan et al., 2013), *35Spro:TPLATE-GFP* (Van Damme et al., 2006), *TMLprpo:TML-YFP* (Gadeyne et al., 2014), *35Spro:DRP1A-GFP* (Konopka and Bednarek, 2008), *DRP1Cpro:DRP1C-GFP* (Konopka et al., 2008), *PIN2pro:PIN2-GFP* (Xu and Scheres, 2005), *35Spro:RCI2A-GFP* (Cutler et al., 2000), *35Spro:sec-GFP* (Zheng et al., 2004), *VHAa1pro:VHAa1-RFP* (Dettmer et al., 2006), *35Spro:SYP41-GFP* (Uemura et al., 2004), and *SYP61pro:SYP61-CFP* (Robert et al., 2008) and estradiol-inducible *ESTRpro:amiR-TPLATE* and *amiR-TML* lines (Gadeyne et al., 2014); clathrin mutants *clc2-1* (SALK_016049; Wang et al., 2013b), *clc3-1* (CS100219; Wang et al., 2013b), *chc1-2* (SALK_103252 from ABRC), *chc2-2* (SALK_042321 from ABRC), *ap1σ1-1* (SALK_145719 from ABRC), *ap1σ2-1* (SALK_049615C from ABRC), *ap1μ2* (CS16318 from ABRC), *ap2σ-1* (SALK_141555; Fan et al., 2013), and *ap2μ-1* (SALK_083693C from ABRC; Wang et al., 2016a).

The construct of *35Spro:AP1σ2-GFP* was generated using PCR, restriction digestion, and ligation into transformation vectors and consequently transformed into the WT accession Columbia-0 (Col-0). Homozygous mutant lines, including *clc*, *chc* (Wang et al., 2013b), *ap-1* (Supplemental Table S1), *ap-2* (Fan et al., 2013; Wang et al., 2016a), and *tpc* (Gadeyne et al., 2014) were isolated and/or identified by PCR- and RT-PCR- or ESTR-based assays, respectively. The *clc2-1 clc3-1*, *chc1-2 chc2-2*, and *ap1σ1-1 ap1σ2-1* double mutants were generated by crossing and verified by genotyping PCR. Fluorescently tagged marker lines were crossed into the *clc*, *chc*, *ap-1*, *ap-2*, and *tpc* mutants, and homozygous lines were confirmed based on their mutant phenotypes, genotyping PCR (Supplemental Table S1), and fluorescence.

Seeds were surface sterilized and stratified for 3 days at 4 °C in the dark and then sown onto half-strength MS medium with 1.5% (w/v) agar, unless otherwise specified. Seedlings were grown vertically on plates in a climate-controlled growth room (22 °C/20 °C day/night temperature, 16-h light/8-h dark photoperiod, and 80 μE s^{-1} m^{-2} light intensity provided by a mixture of cool [3,000K] and warm [6,500K] white LED lamps). Five-day-old seedlings with healthy roots were used in this study.

Chemical solutions and treatments

Unless otherwise specified, all reagents were purchased from Sigma–Aldrich. DMSO was used to dissolve BFA (50 mM), ConcA (5 mM), ES2 (40 mM), ES16 (10 mM), CHX (50 mM), and ESTR (20 mM) for stock solutions. Unless otherwise indicated in the text, final working concentrations were 5 μM for ConcA, 20 μM for ES16 and ESTR, 40 μM for ES2, and 50 μM for CHX and BFA.

All pretreatment and posttreatment time durations are indicated in the text. All pretreatments and treatments were performed as previously described (Wang et al., 2016a). For induction of amiR-TPLATE and amiR-TML, surface-sterilized and stratified seeds were sown onto half-strength MS medium with 1.5% (w/v) agar containing 20 μM ESTR and then grown vertically for 5 days; subsequent liquid treatments also contained 20 μM ESTR. The resulting seedlings were used in live-cell imaging or IF analysis.

Polyclonal antibodies

Polyclonal antibodies (anti-TPLATE and anti-TML) were raised in rabbits using synthesized peptides for each protein (see Supplemental Table S2) coupled with keyhole limpet hemocyanin containing an additional N-terminal Cys (Huabio). Antibodies were affinity purified using immobilized peptide affinity columns, and their specificity was verified as shown in Supplemental Figure S7, A.

IF and live-cell confocal microscopy

Immunolocalization analysis was performed as previously described (Wang et al., 2013b, 2016a). All primary antibodies (Supplemental Table S2) used for immunolocalization were detected using Cy3-labeled anti-rabbit secondary antibodies (1:100 dilution; Sigma–Aldrich Catalog No. C2306). Images were captured using a confocal laser scanning microscope (Leica TCS SP5 AOBS). For imaging Cy3, the 543-nm line of the helium/neon laser was used for excitation, and emission was detected from 550 to 570 nm. For live-cell imaging of CFP, GFP, and YFP, the 458-, 488-, and 514-nm lines of the argon laser were used for excitation, and emission was detected from 460 to 500, from 496 to 532, and from 520 to 560 nm, respectively. For mKO and RFP imaging, the 543- and 594-nm lines of the helium/neon laser were used for excitation, and emission was detected from 560 to 600 and from 612 to 666 nm, respectively. For FM4-64 staining imaging, the 594-nm line of the helium/neon laser was used for excitation, and emission was detected from 651 to 761 nm. For quantitative measurement of fluorescence, all parameters (laser, pinhole, and gain settings) of the confocal microscope were identical among different treatments or genotypes.

To quantify the intensities of fluorescence signals at the PM or intracellular compartments, digital images of root epidermal cells within the division/transition zone were analyzed using ImageJ software (http://rsb.info.nih.gov/ij/; Schindelin et al., 2015). The intracellular signal intensity within individual cells was defined as a region of interest (ROI) subtending the PM. Nuclear regions present within the plane of focus were excluded from the intracellular ROI. To quantify the level of PM signal intensity, ROIs that encompassed the fluorescence signal of the entire cell cortex were assigned. For quantitative analysis of the recycling of internalized PM proteins entrapped in BFA bodies prior to and after BFA washout, non-BFA background signal was subtracted from the intracellular ROI before calculating the ratio of intracellular to PM fluorescent signal intensities.

Localization of TGN/EE-resident proteins after BFA treatment was examined by determining the relative BFA body area per cell. To quantify the relative BFA body area per cell, individual BFA bodies within a single optical section of an epidermal root cell were defined as ROIs and total area of the ROIs divided by the number of BFA bodies per cell was determined using ImageJ.

Confocal FRAP analysis

FRAP assays for GFP-fused proteins were performed on a spinning disk confocal microscope (Zeiss Cell Observer). A ROI (dashed boxes in Figure 10; approximately 5–6 cells/layer) selected with the zoom function was bleached for 1 min at full laser power until reaching the background levels of roots that did not accumulate GFP-fused proteins by scanning. GFP fluorescence was bleached throughout 3–4 cell layers, as monitored by scanning above and below the cells of interest as previously described (Grebe et al., 2003).

For quantification of GFP fluorescence intensities before (pre-bleach) or after bleaching (after-bleach), the fluorescent signal intensities of the ROIs were measured by ImageJ. To compare the rates of GFP fluorescent signal recovery between the WT versus *ap2σ-1* cells or the mock versus estradiol treatments in amiR-*TPLATE*, the fluorescent signal intensities before and 0-min after bleaching were set to 100% and 0%, respectively (Grebe et al., 2003).

Live-cell TIRF microscopy

Seedlings grown vertically were mounted on a glass slide in liquid half-strength MS medium and observed under a TIRF system with an Olympus IX-83 microscope equipped with a 100× oil-immersion objective (numerical aperture 1.49; Olympus). GFP-/YFP-fused proteins were excited with the 488-nm laser line. Time-lapse series images were taken at up to 250 images per sequence and acquired with 200-ms exposure time. Dynamic behaviors including foci densities and lifetimes of fluorescently labeled proteins of interest at the PM were tracked using the MATLAB Graphical User Interface program as previously described (Xue et al., 2018). The kymographs were generated using ImageJ.

Membrane-associated protein isolation and immunoblot analysis

Preparation of total, soluble, and microsomal membrane subcellular protein fractions was as described previously (Abas et al., 2006; Wang et al., 2016a). For immunoblot analysis, the antibodies including anti-CLC1, -CLC2, -CLC3, -CHC, -AP2μ, -AP2σ (Supplemental Table S2), -GFP (1:1,000 dilution; TransGen Biotech Catalog No. HT801-01), anti-RFP (1:1,000 dilution; MBL Biotech Catalog No. M204-3), and anti-SMT1 (1:1,000 dilution; Agrisera Catalog No. AS07266) were used. Band fluorescent signal intensities were quantitated as described previously (Wang et al., 2016a). Coomassie Brilliant Blue (CBB) staining served as a loading control to calculate the relative band fluorescent signal intensities (Wang et al., 2016a). All primary antibodies used in immunoblotting were detected using anti-rabbit or -mouse secondary antibodies (1:50,000 dilution; Huabio Catalog No. HA1019 or HA1009) conjugated to horseradish peroxidase and detected by a chemiluminescent-enhanced substrate kit (Thermo Scientific).

RT-PCR and RT-qPCR assays

The total RNA was isolated using the RNeasy Plant Mini Kit (Qiagen). First-strand cDNA was synthesized with the SuperScript III First-Strand Synthesis System (Invitrogen). The cDNA templates were used in PCR amplification for *AP1σ1* (28 cycles), *AP1σ2* (28 cycles), and *ACTIN 2* (26

cycles; as internal control) transcripts with the gene-specific primers (Supplemental Table S1). The RT-qPCR assay was performed with gene-specific primers (Supplemental Table S3) as described previously (Wang et al., 2016a).

Accession numbers

Sequence data from this article can be found in the Arabidopsis Genome Initiative under the following accession numbers: *CLC1* (At2g20760), *CLC2* (At2g40060), *CLC3* (At3g51890), *CHC1* (At3g11130), *CHC2* (At3g08530), *AP1σ1* (At4g35410), *AP1σ2* (At2g17380), *AP1μ2* (At1g60780), *AP2σ* (At1g47830), *AP2μ* (At5g46630), *TPLATE* (At3g01780), *TML* (At5g57460), *PIN2* (At5g57090), *RCI2A* (At3g05880), *DRP1A* (At5g42080), *DRP1C* (At1g14830), *VHAa1* (At2g28520), *SYP41* (At5g26980), *SYP61* (At1g28490), *UBIQUITIN 7* (At2g35635), and *ACTIN 2* (At3g18780).

Supplemental data

The following materials are available in the online version of this article.

Supplemental Figure S1. Co-localization analysis of AP-1 subunits and clathrin light chain, CLC2.

Supplemental Figure S2. Molecular and phenotypic characterization of *ap1σ1* and *ap1σ2*.

Supplemental Figure S3. GFP-tagged CLC, CHC, and AP1σ2 membrane association in *ap1μ2*.

Supplemental Figure S4. Developmental and endocytic defects in *ap1μ2*.

Supplemental Figure S5. Reduced recycling to the PM of PIN2-GFP and RCI2A-GFP in *ap-1*.

Supplemental Figure S6. Co-localization analysis of internalized FM4-64 and clathrin at the TGN/EE in *ap-1*.

Supplemental Figure S7. Analysis of the specificity of antibodies used for immunodetection studies.

Supplemental Figure S8. Reduction in levels of PM-associated DRP1-GFP in *ap-1*.

Supplemental Figure S9. RT-qPCR analysis of transcriptional levels of endogenous and exogenous core components of CME machinery in *ap1μ2*.

Supplemental Figure S10. Effects of exocytosis/PM recycling inhibitors on TGN/EE marker localization.

Supplemental Figure S11. Inhibitors of exocytosis/PM recycling cause a reduction in levels of membrane-associated clathrin.

Supplemental Figure S12. Inhibitors of exocytosis/PM recycling decrease the levels of PM-associated AP-2/TPC subunits.

Supplemental Figure S13. Immunoblot analysis of effects of exocytosis/PM recycling inhibitors on membrane recruitment of clathrin, AP-2/TPC, and DRP1.

Supplemental Figure S14. Reduced recycling to the PM of RCI2A-GFP in *ap-2* and *tpc*.

Supplemental Figure S15. RT-qPCR analysis of transcriptional levels of *AP-1* and *clathrin* in *ap-2* and *tpc*.

Supplemental Figure S16. Downregulation of *TPLATE* or *TML* mRNA expression reduced the levels of TGN/EE-associated AP-1.

Supplemental Figure S17. Membrane recruitment of clathrin and AP-1 is reduced in *ap-2* and *tpc* mutant seedlings.

Supplemental Figure S18. Localization of TGN/EE markers in *ap-2* and *tpc*.

Supplemental Data Set S1. Summary of statistical analyses.

Supplemental Table S1. PCR primer sequences for genotyping, RT-PCR, and cloning

Supplemental Table S2. Information for antibodies

Supplemental Table S3. RT-qPCR primer sequences

Supplemental Movie S1. TIRF imaging of CLC3-GFP in WT and *ap1μ2*.

Supplemental Movie S2. TIRF imaging of AP2μ-YFP in WT and *ap1μ2*.

Supplemental Movie S3. TIRF imaging of TML-YFP in WT and *ap1μ2*.

References

Abas L, Benjamins R, Malenica N, Paciorek T, Wisniewska J, Moulinier-Anzola JC, Sieberer T, Friml J, Luschnig C (2006) Intracellular trafficking and proteolysis of the *Arabidopsis* auxin-efflux facilitator PIN2 are involved in root gravitropism. Nat Cell Biol **8**: 249–256 (Erratum. Nat Cell Biol **8**: 424)

Bashline L, Li S, Anderson CT, Lei L, Gu Y (2013) The endocytosis of cellulose synthase in *Arabidopsis* is dependent on μ2, a clathrin-mediated endocytosis adaptin. Plant Physiol **163**: 150–160

Boehm CM, Obado S, Gadelha C, Kaupisch A, Manna PT, Gould GW, Munson M, Chait BT, Rout MP, Field MC (2017) The trypanosome exocyst: A conserved structure revealing a new role in endocytosis. PLoS Pathog **13**: e1006063

Bolte S, Talbot C, Boutte Y, Catrice O, Read ND, Satiat Jeunemaitre B (2004) FM-dyes as experimental probes for dissecting vesicle trafficking in living plant cells. J Microsc **214**: 159–173

Boutté Y, Frescatada-Rosa M, Men S, Chow CM, Ebine K, Gustavsson A, Johansson L, Ueda T, Moore I, Juergens G, et al. (2010) Endocytosis restricts *Arabidopsis* KNOLLE syntaxin to the cell division plane during late cytokinesis. EMBO J 29: 546–558

Burgess J, Jauregui M, Tan J, Rollins J, Lallet S, Leventis PA, Boulianne GL, Chang HC, Le Borgne R, Krämer H, et al. (2011) AP-1 and clathrin are essential for secretory granule biogenesis in *Drosophila*. Mol Biol Cell 22: 2094–2105

Casler JC, Papanikou E, Barrero JJ, Glick BS (2019) Maturation-driven transport and AP-1-dependent recycling of a secretory cargo in the Golgi. J Cell Biol 218: 1582–1601

Castillon GA, Burriat-Couleru P, Abegg D, Criado Santos N, Watanabe R (2018) Clathrin and AP1 are required for apical sorting of glycosyl phosphatidyl inositol-anchored proteins in biosynthetic and recycling routes in Madin–Darby canine kidney cells. Traffic 19: 215–228

Cutler SR, Ehrhardt DW, Griffitts JS, Somerville CR (2000) Random GFP::cDNA fusions enable visualization of subcellular structures in cells of *Arabidopsis* at a high frequency. Proc Natl Acad Sci U S A 97: 3718–3723

Daboussi L, Costaguta G, Payne GS (2012) Phosphoinositide-mediated clathrin adaptor progression at the *trans*-Golgi network. Nat Cell Biol 14: 239–248

Day KJ, Casler JC, Glick BS (2018) Budding yeast has a minimal endomembrane system. Dev Cell 44: 56–72.e4

Dejonghe W, Kuenen S, Mylle E, Vasileva M, Keech O, Viotti C, Swerts J, Fendrych M, Ortiz-Morea FA, Mishev K, et al. (2016) Mitochondrial uncouplers inhibit clathrin-mediated endocytosis largely through cytoplasmic acidification. Nat Commun 7: 11710

Deng S, Sun J, Zhao R, Ding M, Zhang Y, Sun Y, Wang W, Tan Y, Liu D, Ma X, et al. (2015) *Populus euphratica* APYRASE2 enhances cold tolerance by modulating vesicular trafficking and extracellular ATP in *Arabidopsis* plants. Plant Physiol 169: 530–548

Dettmer J, Hong-Hermesdorf A, Stierhof YD, Schumacher K (2006) Vacuolar H$^+$-ATPase activity is required for endocytic and secretory trafficking in *Arabidopsis*. Plant Cell 18: 715–730

Dhonukshe P, Aniento F, Hwang I, Robinson DG, Mravec J, Stierhof YD, Friml J (2007) Clathrin-mediated constitutive endocytosis of PIN auxin efflux carriers in *Arabidopsis*. Curr Biol 17: 520–527

Drakakaki G, van de Ven W, Pan S, Miao Y, Wang J, Keinath NF, Weatherly B, Jiang L, Schumacher K, Hicks G, et al. (2012) Isolation and proteomic analysis of the SYP61 compartment reveal its role in exocytic trafficking in *Arabidopsis*. Cell Res 22: 413–424

Fan L, Hao H, Xue Y, Zhang L, Song K, Ding Z, Botella MA, Wang H, Lin J (2013) Dynamic analysis of *Arabidopsis* AP2σ subunit reveals a key role in clathrin-mediated endocytosis and plant development. Development 140: 3826–3837

Feng QN, Kang H, Song SJ, Ge FR, Zhang YL, Li E, Li S, Zhang Y (2016) *Arabidopsis* RhoGDIs are critical for cellular homeostasis of pollen tubes. Plant Physiol 170: 841–856

Fujimoto M, Arimura S, Ueda T, Takanashi H, Hayashi Y, Nakano A, Tsutsumi N (2010) *Arabidopsis* dynamin-related proteins DRP2B and DRP1A participate together in clathrin-coated vesicle formation during endocytosis. Proc Natl Acad Sci U S A 107: 6094–6099

Gadeyne A, Sánchez-Rodríguez C, Vanneste S, Di Rubbo S, Zauber H, Vanneste K, Van Leene J, De Winne N, Eeckhout D, Persiau G, et al. (2014) The TPLATE adaptor complex drives clathrin-mediated endocytosis in plants. Cell 156: 691–704

Gall WE, Geething NC, Hua Z, Ingram MF, Liu K, Chen SI, Graham TR (2002) Drs2p-dependent formation of exocytic clathrin-coated vesicles in vivo. Curr Biol 12: 1623–1627

Geldner N, Anders N, Wolters H, Keicher J, Kornberger W, Muller P, Delbarre A, Ueda T, Nakano A, Juergens G (2003) The *Arabidopsis* GNOM ARF-GEF mediates endosomal recycling, auxin transport, and auxin-dependent plant growth. Cell 112: 219–230

Gendre D, Jonsson K, Boutté Y, Bhalerao RP (2015) Journey to the cell surface—the central role of the trans-Golgi network in plants. Protoplasma 252: 385–398

Gendre D, Oh J, Boutté Y, Best JG, Samuels L, Nilsson R, Uemura T, Marchant A, Bennett MJ, Grebe M, et al. (2011) Conserved *Arabidopsis* ECHIDNA protein mediates *trans*-Golgi-network trafficking and cell elongation. Proc Natl Acad Sci U S A 108: 8048–8053

Gómez-Elías MD, Fissore RA, Cuasnicú PS, Cohen DJ (2020) Compensatory endocytosis occurs after cortical granule exocytosis in mouse eggs. J Cell Physiol 235: 4351–4360

Gravotta D, Carvajal-Gonzalez JM, Mattera R, Deborde S, Banfelder JR, Bonifacino JS, Rodriguez-Boulan E (2012) The clathrin adaptor AP-1A mediates basolateral polarity. Dev Cell 22: 811–823

Gravotta D, Perez Bay A, Jonker CTH, Zager PJ, Benedicto I, Schreiner R, Caceres PS, Rodriguez-Boulan E (2019) Clathrin and clathrin adaptor AP-1 control apical trafficking of megalin in the biosynthetic and recycling routes. Mol Biol Cell 30: 1716–1728

Grebe M, Xu J, Möbius W, Ueda T, Nakano A, Geuze HJ, Rook MB, Scheres B (2003) *Arabidopsis* sterol endocytosis involves actin-mediated trafficking via ARA6-positive early endosomes. Curr Biol 13: 1378–1387

Gurunathan S, Chapman-Shimshoni D, Trajkovic S, Gerst JE (2000) Yeast exocytic v-SNAREs confer endocytosis. Mol Biol Cell 11: 3629–3643

He M, Lan M, Zhang B, Zhou Y, Wang Y, Zhu L, Yuan M, Fu Y (2018) Rab-H1b is essential for trafficking of cellulose synthase and for hypocotyl growth in *Arabidopsis thaliana*. J Integr Plant Biol 60: 1051–1069

Houy S, Estay-Ahumada C, Croisé P, Calco V, Haeberlé AM, Bailly Y, Billuart P, Vitale N, Bader MF, Ory S, et al. (2015) Oligophrenin-1 connects exocytotic fusion to compensatory endocytosis in neuroendocrine cells. J Neurosci 35: 11045–11055

Ito E, Fujimoto M, Ebine K, Uemura T, Ueda T, Nakano A (2012) Dynamic behavior of clathrin in *Arabidopsis thaliana* unveiled by live imaging. Plant J 69: 204–216

Jaiswal JK, Rivera VM, Simon SM (2009) Exocytosis of post-Golgi vesicles is regulated by components of the endocytic machinery. Cell 137: 1308–1319

Johansen J, Alfaro G, Beh CT (2016) Polarized exocytosis induces compensatory endocytosis by Sec4p-regulated cortical actin polymerization. PLoS Biol 14: e1002534

Jose M, Tollis S, Nair D, Mitteau R, Velours C, Massoni-Laporte A, Royou A, Sibarita JB, McCusker D (2015) A quantitative imaging-based screen reveals the exocyst as a network hub connecting endocytosis and exocytosis. Mol Biol Cell 26: 2519–2534

Kaksonen M, Roux A (2018) Mechanisms of clathrin-mediated endocytosis. Nat Rev Mol Cell Biol 19: 313–326

Kawasaki F, Iyer J, Posey LL, Sun CE, Mammen SE, Yan H, Ordway RW (2011) The DISABLED protein functions in clathrin-mediated synaptic vesicle endocytosis and exoendocytic coupling at the active zone. Proc Natl Acad Sci U S A 108: E222–E229

Ketelaar T, Galway ME, Mulder BM, Emons AM (2008) Rates of exocytosis and endocytosis in *Arabidopsis* root hairs and pollen tubes. J Microsc 231: 265–273

Kim SY, Xu ZY, Song K, Kim DH, Kang H, Reichardt I, Sohn EJ, Friml J, Juergens G, Hwang I (2013) Adaptor protein complex 2-mediated endocytosis is crucial for male reproductive organ development in *Arabidopsis*. Plant Cell 25: 2970–2985

Kirchhausen T, Owen D, Harrison SC (2014) Molecular structure, function, and dynamics of clathrin-mediated membrane traffic. Cold Spring Harb Perspect Biol 6: a016725

Kitakura S, Vanneste S, Robert S, Löfke C, Teichmann T, Tanaka H, Friml J (2011) Clathrin mediates endocytosis and polar distribution of PIN auxin transporters in *Arabidopsis*. Plant Cell 23: 1920–1931

Konopka CA, Bednarek SY (2008) Comparison of the dynamics and functional redundancy of the *Arabidopsis* dynamin-related isoforms DRP1A and DRP1C during plant development. Plant Physiol **147**: 1590–1602

Konopka CA, Backues SK, Bednarek SY (2008) Dynamics of *Arabidopsis* dynamin-related protein 1C and a clathrin light chain at the plasma membrane. Plant Cell **20**: 1363–1380

Kukulski W, Picco A, Specht T, Briggs JA, Kaksonen M (2016) Clathrin modulates vesicle scission, but not invagination shape, in yeast endocytosis. eLife **5**: e16036

Lam SK, Cai Y, Tse YC, Wang J, Law AH, Pimpl P, Chan HY, Xia J, Jiang L (2009) BFA-induced compartments from the Golgi apparatus and *trans*-Golgi network/early endosome are distinct in plant cells. Plant J **60**: 865–881

Lam SK, Tse YC, Robinson DG, Jiang L (2007) Tracking down the elusive early endosome. Trends Plant Sci **12**: 497–505

Larson ER, Van Zelm E, Roux C, Marion-Poll A, Blatt MR (2017) Clathrin heavy chain subunits coordinate endo- and exocytic traffic and affect stomatal movement. Plant Physiol **175**: 708–720

Li G, Liang W, Zhang X, Ren H, Hu J, Bennett MJ, Zhang D (2014) Rice actin-binding protein RMD is a key link in the auxin-actin regulatory loop that controls cell growth. Proc Natl Acad Sci U S A **111**: 10377–10382

Li P, Merrill SA, Jorgensen EM, Shen K (2016) Two clathrin adaptor protein complexes instruct axon-dendrite polarity. Neuron **90**: 564–580

Li R, Rodriguez-Furlan C, Wang J, van de Ven W, Gao T, Raikhel NV, Hicks GR (2017) Different endomembrane trafficking pathways establish apical and basal polarities. Plant Cell **29**: 90–108

Martzoukou O, Diallinas G, Amillis S (2018) Secretory vesicle polar sorting, endosome recycling and cytoskeleton organization require the AP-1 complex in *Aspergillus nidulans*. Genetics **209**: 1121–1138

Mayers JR, Hu T, Wang C, Cárdenas JJ, Tan Y, Pan J, Bednarek SY (2017) SCD1 and SCD2 form a complex that functions with the exocyst and RabE1 in exocytosis and cytokinesis. Plant Cell **29**: 2610–2625

McMahon HT, Boucrot E (2011) Molecular mechanism and physiological functions of clathrin-mediated endocytosis. Nat Rev Mol Cell Biol **12**: 517–533

McMichael CM, Reynolds GD, Koch LM, Wang C, Jiang N, Nadeau J, Sack FD, Gelderman MB, Pan J, Bednarek SY (2013) Mediation of clathrin-dependent trafficking during cytokinesis and cell expansion by *Arabidopsis* stomatal cytokinesis defective proteins. Plant Cell **25**: 3910–3925

Meunier FA, Gutiérrez LM (2016) Captivating new roles of F-actin cortex in exocytosis and bulk endocytosis in neurosecretory cells. Trends Neurosci **39**: 605–613

Narasimhan M, Johnson A, Prizak R, Kaufmann WA, Tan S, Casillas-Pérez B, Friml J (2020) Evolutionarily unique mechanistic framework of clathrin-mediated endocytosis in plants. eLife **9**: e52067

Ortiz-Morea FA, Savatin DV, Dejonghe W, Kumar R, Luo Y, Adamowski M, Van den Begin J, Dressano K, Pereira de Oliveira G, Zhao X, et al. (2016) Danger-associated peptide signaling in *Arabidopsis* requires clathrin. Proc Natl Acad Sci U S A **113**: 11028–11033

Otegui M, Staehelin LA (2000) Cytokinesis in flowering plants: more than one way to divide a cell. Curr Opin Plant Biol **3**: 493–502

Otegui MS, Mastronarde DN, Kang BH, Bednarek SY, Staehelin LA (2001) Three-dimensional analysis of syncytial-type cell plates during endosperm cellularization visualized by high resolution electron tomography. Plant Cell **13**: 2033–2051

Paez Valencia J, Goodman K, Otegui MS (2016) Endocytosis and endosomal trafficking in plants. Annu Rev Plant Biol **67**: 309–335

Pantazopoulou A, Glick BS (2019) A kinetic view of membrane traffic pathways can transcend the classical view of Golgi compartments. Front Cell Dev Biol **7**: 153

Papanikou E, Day KJ, Austin J, Glick BS (2015) COPI selectively drives maturation of the early Golgi. eLife **4**: e13232

Park M, Song K, Reichardt I, Kim H, Mayer U, Stierhof YD, Hwang I, Juergens G (2013) *Arabidopsis* μ-adaptin subunit AP1M of adaptor protein complex 1 mediates late secretory and vacuolar traffic and is required for growth. Proc Natl Acad Sci U S A **110**: 10318–10323

Pieperhoff MS, Schmitt M, Ferguson DJ, Meissner M (2013) The role of clathrin in post-Golgi trafficking in *Toxoplasma gondii*. PLoS ONE **8**: e77620

Ravikumar R, Kalbfuß N, Gendre D, Steiner A, Altmann M, Altmann S, Rybak K, Edelmann H, Stephan F, Lampe M, et al. (2018) Independent yet overlapping pathways ensure the robustness and responsiveness of trans-Golgi network functions in *Arabidopsis*. Development **145**: dev169201

Reynolds GD, Wang C, Pan J, Bednarek SY (2018) Inroads into internalization: five years of endocytic exploration. Plant Physiol **176**: 208–218

Riezman H (1985) Endocytosis in yeast: several of the yeast secretory mutants are defective in endocytosis. Cell **40**: 1001–1009

Robert S, Chary SN, Drakakaki G, Li S, Yang Z, Raikhel NV, Hicks GR (2008) Endosidin1 defines a compartment involved in endocytosis of the brassinosteroid receptor BRI1 and the auxin transporters PIN2 and AUX1. Proc Natl Acad Sci U S A **105**: 8464–8469

Samuels AL, Bisalputra T (1990) Endocytosis in elongating root cells of *Lobelia erinus*. J Cell Sci **97**: 157–166

Schindelin J, Rueden CT, Hiner MC, Eliceiri KW (2015) The ImageJ ecosystem: an open platform for biomedical image analysis. Mol Reprod Dev **82**: 518–529

Shimizu Y, Takagi J, Ito E, Ito Y, Ebine K, Komatsu Y, Goto Y, Sato M, Toyooka K, Ueda T, et al. (2021) Cargo sorting zones in the *trans*-Golgi network visualized by super-resolution confocal live imaging microscopy in plants. Nat Commun **12**: 1901

Sommer B, Oprins A, Rabouille C, Munro S (2005) The exocyst component Sec5 is present on endocytic vesicles in the oocyte of *Drosophila melanogaster*. J Cell Biol **169**: 953–963

Song J, Lee MH, Lee GJ, Yoo CM, Hwang I (2006) *Arabidopsis* EPSIN1 plays an important role in vacuolar trafficking of soluble cargo proteins in plant cells via interactions with clathrin, AP-1, VTI11, and VSR1. Plant Cell **18**: 2258–2274

Stamnes M (2002) Regulating the actin cytoskeleton during vesicular transport. Curr Opin Cell Biol **14**: 428–433

Teh OK, Shimono Y, Shirakawa M, Fukao Y, Tamura K, Shimada T, Hara-Nishimura I (2013) The AP-1 μ adaptin is required for KNOLLE localization at the cell plate to mediate cytokinesis in *Arabidopsis*. Plant Cell Physiol **54**: 838–847

Uemura T, Ueda T, Ohniwa RL, Nakano A, Takeyasu K, Sato MH (2004) Systematic analysis of SNARE molecules in *Arabidopsis*: dissection of the post-Golgi network in plant cells. Cell Struct Funct **29**: 49–65

Van Damme D, Coutuer S, De Rycke R, Bouget FY, Inzé D, Geelen D (2006) Somatic cytokinesis and pollen maturation in *Arabidopsis* depend on TPLATE, which has domains similar to coat proteins. Plant Cell **18**: 3502–3518

Wang C, Hu T, Yan X, Meng T, Wang Y, Wang Q, Zhang X, Gu Y, Sánchez-Rodríguez C, Gadeyne A, et al. (2016a) Differential regulation of clathrin and its adaptor proteins during membrane recruitment for endocytosis. Plant Physiol **171**: 215–229

Wang C, Yan X, Chen Q, Jiang N, Fu W, Ma B, Liu J, Li C, Bednarek SY, Pan J (2013b) Clathrin light chains regulate clathrin-mediated trafficking, auxin signaling, and development in *Arabidopsis*. Plant Cell **25**: 499–516

Wang JG, Feng C, Liu HH, Ge FR, Li S, Li HJ, Zhang Y (2016b) HAPLESS13-mediated trafficking of STRUBBELIG is critical for ovule development in *Arabidopsis*. PLoS Genet **12**: e1006269

Wang JG, Li S, Zhao XY, Zhou LZ, Huang GQ, Feng C, Zhang Y (2013a) HAPLESS13, the *Arabidopsis* μ1 adaptin, is essential for

protein sorting at the trans-Golgi network/early endosome. Plant Physiol **162:** 1897–1910

Watanabe S, Rost BR, Camacho-Pérez M, Davis MW, Söhl-Kielczynski B, Rosenmund C, Jorgensen EM (2013) Ultrafast endocytosis at mouse hippocampal synapses. Nature **504:** 242–247

Wu W, Xu J, Wu XS, Wu LG (2005) Activity-dependent acceleration of endocytosis at a central synapse. J Neurosci **25:** 11676–11683

Xu J, Scheres B (2005) Dissection of *Arabidopsis* ADP-RIBOSYLATION FACTOR 1 function in epidermal cell polarity. Plant Cell **17:** 525–536

Xue Y, Xing J, Wan Y, Lv X, Fan L, Zhang Y, Song K, Wang L, Wang X, Deng X, **et al.** (2018) *Arabidopsis* blue light receptor phototropin 1 undergoes blue light-induced activation in membrane microdomains. Mol Plant **11:** 846–859

Yamaoka S, Shimono Y, Shirakawa M, Fukao Y, Kawase T, Hatsugai N, Tamura K, Shimada T, Hara-Nishimura I (2013) Identification and dynamics of *Arabidopsis* adaptor protein-2 complex and its involvement in floral organ development. Plant Cell **25:** 2958–2969

Zhang C, Brown MQ, van de Ven W, Zhang ZM, Wu B, Young MC, Synek L, Borchardt D, Harrison R, Pan S, et al. (2016) Endosidin2 targets conserved exocyst complex subunit EXO70 to inhibit exocytosis. Proc Natl Acad Sci U S A **113:** E41–E50

Zhang L, Xing J, Lin J (2019) At the intersection of exocytosis and endocytosis in plants. New Phytol **224:** 1479–1489

Zhang Y, Persson S, Hirst J, Robinson MS, van Damme D, Sánchez-Rodríguez C (2015) Change your TPLATE, change your fate: plant CME and beyond. Trends Plant Sci **20:** 41–48

Zheng H, Kunst L, Hawes C, Moore I (2004) A GFP-based assay reveals a role for RHD3 in transport between the endoplasmic reticulum and Golgi apparatus. Plant J **37:** 398–414

Zouhar J, Sauer M (2014) Helping hands for budding prospects: ENTH/ANTH/VHS accessory proteins in endocytosis, vacuolar transport, and secretion. Plant Cell **26:** 4232–4244

Zwiewka M, Nodzyński T, Robert S, Vanneste S, Friml J (2015) Osmotic stress modulates the balance between exocytosis and clathrin-mediated endocytosis in *Arabidopsis thaliana*. Mol Plant **8:** 1175–1187